Rose-Hulman Undergraduate Mathematics Journal

Volume 24
Issue 1

Article 4

A Note On The Involutive Concordance Invariants For Certain (1,1)-Knots

Anna Antal
Yale University, anna.antal@rutgers.edu

Sarah Pritchard
Georgia Institute of Technology, sarah.pritchard@gatech.edu

A Note On The Involutive Concordance Invariants For Certain (1,1)-Knots

Cover Page Footnote

This project was carried out during the Rutgers DIMACS REU in Summer 2021; we thank the organizers of the REU for their support and Kristen Hendricks and Karuna Sangam for supervising this project. We are also grateful to Zipei Nie for sending us his Python code to compute the knot Floer homology of (1,1)-knots. Both authors were supported by NSF CAREER Grant DMS-2019396.

ℝose-Hulman Undergraduate Mathematics Journal
VOLUME 24, ISSUE 1, 2023

A note on the involutive concordance invariants for certain (1,1)-knots

By *Anna Antal* and *Sarah Pritchard*

Abstract. We compute the involutive concordance invariants for the 10- and 11-crossing (1,1)-knots.

1 Introduction

A knot is a smooth embedding of a circle in S^3. Knots are interesting because of their applications to real world problems and in higher-dimensional topology. Knots are often studied via knot invariants; a knot invariant is a simpler algebraic object (such as a number or polynomial) which is associated to each knot. In this paper, we give computations of two relatively new knot invariants for a particular family of knots. We begin by giving a broad overview of this work, then further exposit knots and the knot invariants we work with in the background sections to follow.

Heegaard Floer homology is a suite of invariants of 3-manifolds, knots, and links introduced in the early 2000's by P. Ozsváth and Z. Szabó [OS04b, OS04a], and in the knot case independently by J. Rasmussen [Ras03]. In the knot variant, Heegaard Floer homology associates to a knot K a $\mathbb{Z}\oplus\mathbb{Z}$-filtered, $\mathbb{Z}$-graded chain complex over $\mathbb{F}_2[U,U^{-1}]$ called $CFK^\infty(K)$. Many classical knot invariants can be recovered from this chain complex. For example, $CFK^\infty(K)$ contains the data of the Alexander polynomial [OS04b], the knot genus [OS06], and whether a knot is fibred [Ghi08, Ni07].

We work with involutive Heegaard Floer homology, developed by K. Hendricks and C. Manolescu in 2015 [HM17] as a refinement to Heegaard Floer homology. In the knot version, involutive Heegaard Floer homology additionally considers a skew-filtered automorphism

$$\iota_K : CFK^\infty(K) \to CFK^\infty(K),$$

which is order four up to filtered chain homotopy. Using this supplementary information, involutive Heegaard Floer homology introduced two new knot concordance invariants, $\underline{V}_0(K)$ and $\overline{V}_0(K)$, which are variants of an existing concordance invariant $V_0(K)$ from Heegaard Floer homology. The involutive concordance invariants are interesting because unlike other concordance invariants arising from Heegaard Floer homology such as τ,ϵ,

Mathematics Subject Classification. 57K18
Keywords. Concordance, Knot Theory, Heegaard Floer Homology

and ν, they do not necessarily vanish on knots of finite concordance order such as the figure-eight knot [HM17]. Hendricks and Manolescu give combinatorial computations of the involutive concordance invariants for L-space knots (which include the torus knots) and thin knots (which include alternating and quasi-alternating knots).

Following a similar, but slightly more refined, strategy to Hendricks and Manolescu's computation for thin knots [HM17, Section 8], in this note we compute the involutive concordance invariants $\underline{V}_0(K)$ and $\overline{V}_0(K)$ for all 10 and 11-crossing (1,1)-knots that are neither L-space nor thin. We also include the values of the ordinary concordance invariant $V_0(K)$ for each knot, for easy comparison. Our computations appear in Section 7. Taken together they confirm the following.

Theorem 1.1. For any 10- or 11-crossing (1,1)-knot K, the skew-filtered chain homotopy equivalence class of ι_K, and therefore the value of the concordance invariants $\underline{V}_0(K)$ and $\overline{V}_0(K)$, is determined by $CFK^\infty(K)$.

Organization

This paper is organized as follows. In Section 2, we provide some background on knots and concordance. In Section 3 we provide necessary background on homological algebra; in particular, we discuss general chain complexes in Section 3.1, filtered chain complexes in Section 3.2, bigraded chain complexes in Section 3.3, the Euler characteristic of a chain complex in Section 3.4, and $\mathbb{F}_2[U,U^{-1}]$ complexes in Section 3.5. In Section 4 we briefly introduce Heegaard Floer homology and involutive Heegaard Floer homology; specifically, in Section 4.1 we review the definition of the chain complex $CFK^\infty(K)$ and the concordance invariant $V_0(K)$, and in Section 4.2 we summarize the properties of the map ι_K and the definitions of the involutive concordance invariants $\underline{V}_0(K)$ and $\overline{V}_0(K)$. In Section 5 we discuss parameterizations of (1,1)-knots and Heegaard diagrams. We provide some example computations of the involutive concordance invariants in Section 6; Section 6.1 outlines the computation for the knot $11n_{57}$, and Section 6.2 outlines the computation for the knot 10_{161}. Then, in Section 7 we provide a list of involutive concordance invariants for some 10- and 11-crossing (1,1)-knots for which they were not previously known, along with some amendments to the literature.

2 Knots and Concordance

2.1 Knots

We begin by introducing knots, and going over some useful properties and types of knots.

Definition 2.1. A *knot* is a smooth embedding $K : S^1 \hookrightarrow S^3$ up to isotopy.

Knots are represented by knot diagrams, which are defined as follows.

Definition 2.2. A *knot diagram* for a knot K is a projection of K onto $\mathbb{R}^2$ that has finitely many double points, and has crossing information at each double point.

Some examples of knot diagrams are shown in Figure 1 and 2.

Definition 2.3. The *crossing number* of a knot K is the minimal number of crossings appearing in any diagram of K.

The standard enumeration of knots gives them labels referencing their crossing number. For example, the figure-eight knot 4_1, shown in Figure 1, has crossing number 4.

Definition 2.4. A knot K is *alternating* if there exists a diagram of K such that one can trace along the diagram and pass through alternating over-crossings and under-crossings until returning to the starting point.

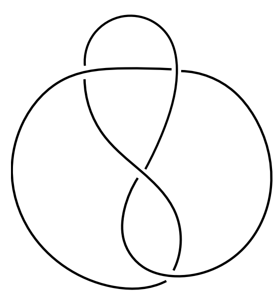

Figure 1: The figure-eight knot 4_1 is an alternating knot with crossing number 4.

Definition 2.5. The (p, q)-*torus knot* is a knot $T_{p,q}$ for coprime p, q that sits on the surface of the torus as described by a map $S^1 \to S^1 \times S^1 \subseteq S^3$ given by $z \mapsto (z^p, z^q)$.

An example of a torus knot is the trefoil, denoted $T_{(2,3)}$, shown in Figure 2. Later, we will discuss L-space knots and thin knots, which share some algebraic properties with torus knots and alternating knots respectively.

We also consider the mirror of a knot, defined as follows.

Definition 2.6. Given a knot K, its *mirror* is a knot $\overline{K}$, which is K with over-crossings changed to under-crossings and vice versa.

Knots do not naively form a group, but there is an operation on knots; we can take a connected sum.

Figure 2: Both the right-handed trefoil knot $3_1 = T_{(2,3)}$, shown on the right, and its mirror the left-handed trefoil on the left are alternating torus knots.

Definition 2.7. Let J, K be two oriented knots. The *connected sum* of J and K, denoted $J\#K$, is constructed by removing a trivial arc (that is, untangled in a three ball) from both J, K and connecting the four endpoints with two new oriented trivial strands in a way that respects the orientations of J and K.

The connect sum of the right-handed trefoil and its mirror the left-handed trefoil is shown in Figure 3.

2.2 Concordance

The invariants computed in this note are a type of knot concordance invariant. Concordance is an equivalence relation on knots; its definition is as follows.

Definition 2.8. Two knots K_1 and K_2 are *concordant* if they co-bound a smooth, properly embedded cylinder in $S^3 \times [0,1]$.

We may consider knots equivalent up to concordance. A knot that is concordant to the unknot is called *slice*. Furthermore, the set of knots in S^3 modulo concordance equipped with the operation induced by connected sum is a group.

2.3 $(1,1)$-Knots

In this paper we will be particularly interested in knots that satisfy a certain simplicity condition, called being $(1,1)$. The definition of a $(1,1)$-knot is as follows.

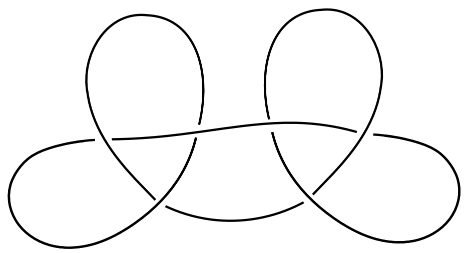

Figure 3: The connected sum of the trefoil and its mirror is denoted $3_1\#\overline{3}_1$.

Definition 2.9. A knot K is a (g,b) knot for $g,b \in \mathbb{Z}$ if it has a diagram on the genus g orientable surface Σ_g composed of b trivial arcs called overpasses and b trivial arcs called underpasses, positioned such that:

1. Overpasses do not intersect each other.
2. Underpasses do not intersect each other.
3. When an overpass meets an underpass, the overpass crosses above the underpass.

A $(1,1)$-knot is a (g,b) knot where $g=1$ and $b=1$. In more detail, a $(1,1)$-knot is a union of two trivial arcs in the standard decomposition of S^3 into two solid tori, one in each torus, such that the arcs share a boundary consisting of two points in the torus $S^1 \times S^1$, which is the mutual boundary of the two solid tori. In Section 5, we discuss algebraic invariants associated to $(1,1)$-knots in more detail.

3 Homological Algebra

3.1 General chain complexes

In this section we review some concepts from homological algebra. First we introduce chain complexes and the maps between them.

Definition 3.1. A *chain complex* over a ring R is a sequence of R-modules (C_i, ∂_i),

$$\cdots \xrightarrow{\partial_3} C_2 \xrightarrow{\partial_2} C_1 \xrightarrow{\partial_1} C_0 \xrightarrow{\partial_0} C_{-1} \xrightarrow{\partial_{-1}} \cdots$$

with the property that $\partial_{i-1} \circ \partial_i = 0$. We call ∂_i the differential map.

Definition 3.2. The i^{th} *homology* of a chain complex (C_i, ∂_i) is

$$H_i(C) = \mathrm{Ker}(\partial_i)/\mathrm{Im}(\partial_{i+1}),$$

where $\mathrm{Ker}(\partial_i)$ denotes the kernel of ∂_i, $\mathrm{Im}(\partial_{i+1})$ denotes the image of ∂_{i+1}, and $C = \bigoplus_{i\in\mathbb{Z}} C_i$ is the graded module.

Example 3.3. Let $\mathbb{F}_2\langle x_1, x_2, \cdots, x_n\rangle$ denote the vector space with basis elements x_i, for $1 \le i \le n$, over the field $\mathbb{F}_2 = \{0,1\}$. Let $C = (C_i, \partial_i)$ be the following chain complex:

$$\begin{array}{ccccccccc} C_3 & & C_2 & & C_1 & & C_0 & & C_{-1} \\ 0 & \xrightarrow{\partial_3} & \mathbb{F}_2\langle e, g\rangle & \xrightarrow{\partial_2} & \mathbb{F}_2\langle a, b, c\rangle & \xrightarrow{\partial_1} & \mathbb{F}_2\langle v\rangle & \xrightarrow{\partial_0} & 0 \end{array}$$

We take $C_i = 0$ for $i \ge 3$ and $i \le -1$. Here, ∂_0 and ∂_3 are both the zero map. We define the maps ∂_1 and ∂_2 on the basis elements of C_1 and C_2, respectively: $\partial_1(a) = \partial_1(b) = \partial_1(c) = 0$, and $\partial_2(e) = \partial_2(f) = a + b + c$. The i^{th} homology of this chain complex for $i \in \{0,1,2\}$ is as follows.

$$\begin{aligned} H_0(C) &= \mathrm{Ker}(\partial_0)/\mathrm{Im}(\partial_1) = \mathbb{F}_2\langle v\rangle/\{0\} = \mathbb{F}_2\langle [v]\rangle. \\ H_1(C) &= \mathrm{Ker}(\partial_1)/\mathrm{Im}(\partial_2) = \mathbb{F}_2\langle a, b, c\rangle/\mathbb{F}_2\langle a+b+c\rangle = \mathbb{F}_2\langle [a], [b]\rangle. \\ H_2(C) &= \mathrm{Ker}(\partial_2)/\mathrm{Im}(\partial_3) = \mathbb{F}_2\langle e+g\rangle/\{0\} = \mathbb{F}_2\langle [e+g]\rangle. \end{aligned}$$

For all other values of i, the homology is trivial.

Definition 3.4. Let (C_i, ∂_{C_i}) and (D_i, ∂_{D_i}) be two chain complexes. A *(graded) chain map* f is a map of modules $f : C_i \to D_i$ with the property that $f \circ \partial_{C_i} = \partial_{D_i} \circ f$.

Definition 3.5. Given chain complexes (C_i, ∂_{C_i}) and (D_i, ∂_{D_i}), two chain maps $f, g : C_i \to D_i$ are *chain homotopic* if there is a map $H : C_i \to D_{i+1}$ with the property that $\partial H + H\partial = f - g$. We write $f \sim g$.

Definition 3.6. Two chain complexes (C_i, ∂_{C_i}) and (D_i, ∂_{D_i}) are *chain homotopy equivalent* if there exist chain maps $f : C_i \to D_i$ and $g : D_i \to C_i$ with the property that $f \circ g \sim \mathrm{Id}_D$ and $g \circ f \sim \mathrm{Id}_C$, where $C = \bigoplus_{i\in\mathbb{Z}} C_i$ and $D = \bigoplus_{i\in\mathbb{Z}} D_i$, and Id_C and Id_D denote the identity maps on C and D, respectively.

We now state a definition that is necessary for our discussion of involutive concordance invariants in section 4.2.

Definition 3.7. Let (C, ∂_C) and (D, ∂_D) be chain complexes and $f : C \to D$ be a (grading-preserving) chain map. The *mapping cone* of f is the complex

$$\mathrm{Cone}(f) = \left(C[-1] \oplus D, \begin{pmatrix} \partial_C & 0 \\ f & \partial_D \end{pmatrix} \right).$$

The term $C[-1]$ means that we are considering the complex C with the homological grading of all elements increased by 1.

3.2 Filtered chain complexes

To discuss filtered chain complexes we must first define a filtration.

Definition 3.8. A *filtration* $\mathscr{F}$ of an algebraic object S is an indexed family $(\mathrm{S}_i)_{i\in\mathrm{I}}$ of sub-objects, for I an ordered set, such that if $i \leq j$, then $\mathrm{S}_i \subseteq \mathrm{S}_j$, and $\mathrm{S} = \cup_{i\in\mathrm{I}}\mathrm{S}_i$.

Now, we have the following restrictions to the definitions above:

Definition 3.9. A *filtered chain complex* is a chain complex (C, ∂), filtered as a vector space with a filtration $\mathscr{F}$ such that $\partial(\mathscr{F}_i) \subseteq \mathscr{F}_i$.

Example 3.10. Consider the following complex (C, ∂):

$$0 \xleftarrow{\partial} \mathbb{F}_2\langle a\rangle \xleftarrow{\partial} \mathbb{F}_2\langle b, d, e, f\rangle \xleftarrow{\partial} \mathbb{F}_2\langle c\rangle$$

Here (and for other filtered chain complexes) we suppress the homological grading of the basis elements in favor of their filtration level. The homological gradings of the basis elements are as follows: a, b, f have homological grading 0, and c, d, e have homological grading 1. The filtration levels of C are as follows: $\mathscr{F}_{-1} = \mathbb{F}_2\langle a\rangle$, $\mathscr{F}_0 = \mathbb{F}_2\langle a, b, d, e, f\rangle$, and $\mathscr{F}_1 = \mathbb{F}_2\langle a, b, c, d, e, f\rangle$. For $i \leq -2, \mathscr{F}_i = \{0\}$. For $i \geq 2, \mathscr{F}_i = \mathbb{F}_2\langle a, b, c, d, e, f\rangle$. The differential map ∂ acts on the basis elements in the following way: $\partial(a) = \partial(b) = \partial(f) = 0$, $\partial(c) = b$, $\partial(d) = f$, and $\partial(e) = a$. The homology of the filtered chain complex is: $\mathrm{H}_*(\mathrm{C}) = \mathrm{Ker}(\partial)/\mathrm{Im}(\partial) = \mathbb{F}_2\langle a, b, f\rangle/\mathbb{F}_2\langle a, b, f\rangle = \{0\}$.

Definition 3.11. Given a chain complex (C, ∂) equipped with a filtration $\mathscr{F}$, the *associated graded complex* is a chain complex given by $\bigoplus_{i\in\mathbb{Z}}\mathscr{F}_i/\mathscr{F}_{i-1}$, taking the direct sum of the quotient complexes together.

Definition 3.12. A *chain map of filtered chain complexes* $(\mathrm{C}, \partial_\mathrm{C})$ and $(\mathrm{D}, \partial_\mathrm{D})$ with filtration $\mathscr{F}$ is a chain map $\Psi : \mathrm{C} \to \mathrm{D}$ such that $\Psi(\mathscr{F}_i) \subseteq \mathscr{F}_i$.

Definition 3.13. A *filtered chain homotopy equivalence* between filtered chain maps $\Psi, \Phi : \mathrm{C} \to \mathrm{D}$ with filtration $\mathscr{F}$ is a map $\mathrm{H} : \mathrm{C} \to \mathrm{D}$ such that $\partial\mathrm{H} + \mathrm{H}\partial = \Psi - \Phi$ and $\mathrm{H}(\mathscr{F}_i) \subseteq \mathscr{F}_i$.

Definition 3.14. Two filtered chain complexes $(\mathrm{C}_i, \partial_{\mathrm{C}_i})$ and $(\mathrm{D}_i, \partial_{\mathrm{D}_i})$ are *filtered chain homotopy equivalent* if there exist chain maps $f : \mathrm{C}_i \to \mathrm{D}_i$ and $g : \mathrm{D}_i \to \mathrm{C}_i$ with the property that $f \circ g \sim \mathrm{Id}_\mathrm{D}$ and $g \circ f \sim \mathrm{Id}_\mathrm{C}$, where $\mathrm{C} = \bigoplus_{i\in\mathbb{Z}}\mathrm{C}_i$ and $\mathrm{D} = \bigoplus_{i\in\mathbb{Z}}\mathrm{D}_i$, and Id_C and Id_D denote the identity maps on C and D, respectively.

Definition 3.15. Let (C, ∂) and (D, ∂) be chain complexes equipped with a $(\mathbb{Z} \oplus \mathbb{Z})$-filtration $\mathscr{F}$, which has a partial order given by $(i_1, j_1) \leq (i_2, j_2)$ if $i_1 \leq i_2$ and $j_1 \leq j_2$. Then, $\Psi : \mathrm{C} \to \mathrm{D}$ is a *skew-filtered chain map* if it is a chain map and $\Psi(\mathscr{F}_{(i,j)}) \subseteq \mathscr{F}_{(j,i)}$ for all $i, j \in \mathbb{Z}$.

Example 3.16. Let (C,∂) be the following $(\mathbb{Z}\oplus\mathbb{Z})$-filtered chain complex.

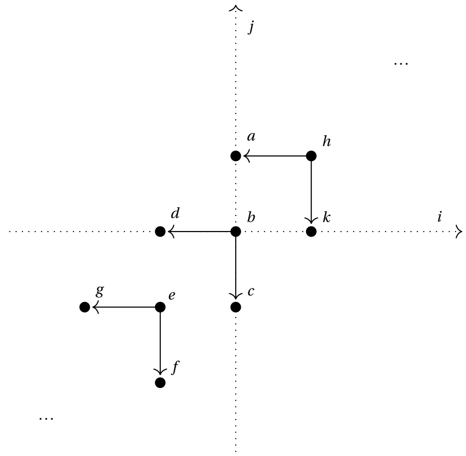

The dots in the picture, for instance the ones labelled by $a, b,$ and c, are basis elements of the vector space C. The arrows between the basis elements denote the map ∂. For example, $\partial(b) = c + d$. The filtration level $\mathscr{F}_{(0,0)}$ consists of everything in the third quadrant of the complex. Thus, $\mathbb{F}_2\langle b,c,d,e,f,g\rangle \subset \mathscr{F}_{(0,0)}$. Also note that reflection along the line $i = j$ is a skew-filtered chain map on the complex.

3.3 Bigraded chain complexes

Definition 3.17. A *bigraded chain complex* is a complex $\mathrm{C} = \bigoplus_{i,j\in\mathbb{Z}} \mathrm{C}_{i,j}$ with the property $\partial_i : \mathrm{C}_{i,j} \to \mathrm{C}_{i-1,j}$. Equivalently, this is a direct sum of chain complexes:

$$\begin{array}{c}
\vdots \\
\cdots \longrightarrow \mathrm{C}_{2,2} \longrightarrow \mathrm{C}_{1,2} \longrightarrow \mathrm{C}_{0,2} \longrightarrow \mathrm{C}_{-1,2} \longrightarrow \mathrm{C}_{-2,2} \longrightarrow \cdots \\
\cdots \longrightarrow \mathrm{C}_{2,1} \longrightarrow \mathrm{C}_{1,1} \longrightarrow \mathrm{C}_{0,1} \longrightarrow \mathrm{C}_{-1,1} \longrightarrow \mathrm{C}_{-2,1} \longrightarrow \cdots \\
\cdots \longrightarrow \mathrm{C}_{2,0} \longrightarrow \mathrm{C}_{1,0} \longrightarrow \mathrm{C}_{0,0} \longrightarrow \mathrm{C}_{-1,0} \longrightarrow \mathrm{C}_{-2,0} \longrightarrow \cdots \\
\vdots
\end{array}$$

Table 1: $\mathrm{H}_{i,j}(\mathrm{C})$

	$i=2$	$i=1$	$i=0$
$j=2$	0	0	$\mathbb{F}_2\langle[n]\rangle$
$j=1$	$\mathbb{F}_2\langle[d+e]\rangle$	$\mathbb{F}_2\langle[k],[l]\rangle$	0
$j=0$	0	$\mathbb{F}_2\langle[a+b]\rangle$	0

Example 3.18. The following complex $(\mathrm{C},\partial) = (\mathrm{C}_{i,j},\partial_{i,j})$ is an example of a bigraded chain complex.

$$\begin{array}{ccccccccc}
 & i=2 & & i=1 & & i=0 & & i=-1 \\
j=2 & 0 & \xrightarrow{\partial} & 0 & \xrightarrow{\partial} & \mathbb{F}_2\langle n\rangle & \xrightarrow{\partial} & 0 \\
j=1 & \mathbb{F}_2\langle d,e\rangle & \xrightarrow{\partial} & \mathbb{F}_2\langle k,l,m\rangle & \xrightarrow{\partial} & 0 & \xrightarrow{\partial} & 0 \\
j=0 & 0 & \xrightarrow{\partial} & \mathbb{F}_2\langle a,b\rangle & \xrightarrow{\partial} & \mathbb{F}_2\langle c\rangle & \xrightarrow{\partial} & 0
\end{array}$$

We view the bigraded chain complex as the direct sum of chain complexes, where the chain complexes are indexed by j, and the vector spaces in each chain complex are indexed by i. The differential map ∂ is defined as follows: $\partial(a) = \partial(b) = c$, $\partial(c) = \partial(n) = 0$, and $\partial(d) = \partial(e) = k + l + m$.
We summarize the homology $\mathrm{H}_{i,j}(\mathrm{C})$ of the complex above in Table 1.

3.4 Euler characteristics

Definition 3.19. The *Euler characteristic* of a chain complex (C,∂) of vector spaces is

$$\sum_{i\in\mathbb{Z}}(-1)^i\dim\big(\mathrm{H}_i(\mathrm{C})\big) = \sum_{i\in\mathbb{Z}}(-1)^i\dim(\mathrm{C}_i).$$

This number is written $\chi(\mathrm{C})$.

Definition 3.20. The *Euler characteristic of a bigraded chain complex* $(\mathrm{C},\partial) = (\mathrm{C}_{i,j},\partial_{i,j})$ is a polynomial

$$\chi(\mathrm{C}_{i,j}) = \sum_{i,j\in\mathbb{Z}}(-1)^i\dim\big(\mathrm{H}_{i,j}(\mathrm{C})\big)\mathrm{T}^j$$

$$= \sum_{i,j \in \mathbb{Z}} (-1)^i \dim(C_{i,j}) T^j$$
$$= \sum_{i,j \in \mathbb{Z}} \chi(C_{i,j}) T^j.$$

Example 3.21. The Euler characteristic of the complex $(C_{i,j}, \partial_{i,j})$ given in Example 3.18 is as follows:

$$\chi(C_{i,j}) = \sum_{i,j \in \mathbb{Z}} \chi(C_{i,j}) T^j = T^2 - T - 1.$$

3.5 $\mathbb{F}_2[U, U^{-1}]$ complexes

We will be interested in $(\mathbb{Z} \oplus \mathbb{Z})$-filtered chain complexes (C, ∂) over the ring $\mathbb{F}_2[U, U^{-1}]$ which are finitely generated and free. Concretely, this means that as a module C is generated by some finite number of elements $x_1, x_2, \cdots, x_m$. Any element of the form $U^n x_i$ is an element of C for $n \in \mathbb{Z}$ and $1 \le i \le m$. In out complexes, multiplication by U will lower the homological grading of an element by 2, and decrease each filtration level of the element by 1. For example, if $x \in C$, x has homological grading a, and $x \in \mathscr{F}_{(i,j)}$, then Ux has homological grading $a-2$, and $Ux \in \mathscr{F}_{(i-1,j-1)}$. Furthermore, the differential map ∂ is U-equivariant, which means that $\partial(U^n x) = U^n \partial x$ for all $n \in \mathbb{Z}$. Any chain map or chain homotopy on $\mathbb{F}_2[U, U^{-1}]$ complexes is also U-equivariant.

Example 3.22. Let (C, ∂) be the following $\mathbb{F}_2[U, U^{-1}]$ complex:

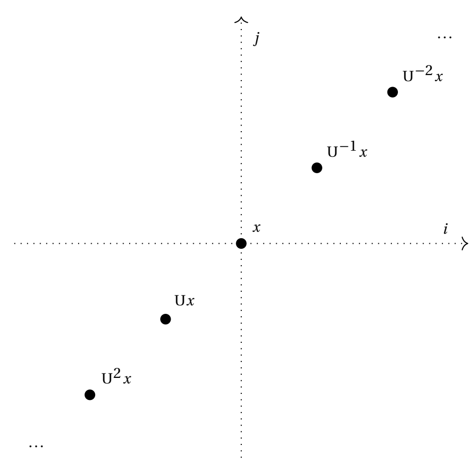

The complex has elements of the form $U^n x$ for $n \in \mathbb{Z}$. The differential ∂ is identically 0 on C. The homological grading of x is 0. Thus, the homological grading of $U^n x$ is $-2n$. Also note that $x \in \mathscr{F}_{(0,0)}$, so $U^n x \in \mathscr{F}_{(-n,-n)}$.

4 Heegaard Floer homology and involutive Heegaard Floer homology

4.1 The chain complex $\mathrm{CFK}^\infty(K)$

We now introduce the complex $\mathrm{CFK}^\infty(K)$ abstractly; in Section 5 we will go over its construction in a special case. To a knot K, Heegaard Floer homology [OS04a, OS04b] associates a $(\mathbb{Z}\oplus\mathbb{Z})$-filtered, $\mathbb{Z}$-graded chain complex $\mathrm{CFK}^\infty(K)$ over $\mathbb{F}_2[U,U^{-1}]$. (Strictly speaking, the construction of $\mathrm{CFK}^\infty(K)$ involves some choices which produce chain complexes which are chain homotopy equivalent via canonical chain homotopies; here and throughout, we will take some model for this chain homotopy equivalence class.)

For the mirror image $\overline{K}$ of a knot K, $\mathrm{CFK}^\infty(\overline{K}) = \mathrm{Hom}_{\mathbb{F}_2[U,U^{-1}]}(\mathrm{CFK}^\infty(K),\mathbb{F}_2[U,U^{-1}])$, the dual of $\mathrm{CFK}^\infty(K)$ over the field $\mathbb{F}_2[U,U^{-1}]$. We can describe the horizontal and vertical components of ∂ in following way:

Definition 4.1. Decompose the differential ∂ on $CFK^\infty(K)$ as

$$\partial = \sum_{i,j\in\mathbb{N}} \partial_{ij},$$

where ∂_{ij} lowers the horizontal grading by i and the vertical grading by j. Then the horizontal and vertical differentials are

$$\partial_{\mathrm{horz}} = \sum_i \partial_{i0}$$

and

$$\partial_{\mathrm{vert}} = \sum_j \partial_{0j}.$$

Given $S \subseteq \mathbb{Z}\oplus\mathbb{Z}$, we let $C\{S\} \subseteq \mathrm{CFK}^\infty(K)$ denote the set of elements with planar gradings in S; if this is closed under ∂ it is a subcomplex of $\mathrm{CFK}^\infty(K)$. The following complexes are important examples:

Definition 4.2. The quotient complexes $C\{i=0\}$ and $C\{j=0\}$ are

$$C\{i=0\} = C\{(i,j) : i \le 0\}/C\{(i,j) : i < 0\}$$

and

$$C\{j=0\} = C\{(i,j) : j \le 0\}/C\{(i,j) : j < 0\}.$$

Since both $C\{(i,j) : i \le 0\}$ and $C\{(i,j) : i < 0\}$ are subcomplexes of $\mathrm{CFK}^\infty(K)$, their quotient is a chain complex. In the same way, $C\{j=0\}$ is a subcomplex also. The Euler characteristic of the associated graded of $C\{i=0\}$ for a knot K is the Alexander polynomial $\Delta_K(t)$. Additionally, the homology of the subcomplex $C\{i=0\}$ equipped with the boundary map ∂_{vert} is

$$H_*\big(C\{i=0\},\partial_{\mathrm{vert}}\big) = \mathbb{F}_{(0)}.$$

Likewise,

$$H_*\big(C\{j=0\},\partial_{\mathrm{horz}}\big)=\mathbb{F}_{(0)}.$$

We are furthermore interested in the subcomplex A_0^-, which has the following definition:

Definition 4.3. The subcomplex A_0^- is defined by

$$A_0^- = C\{(i,j) : i,j \le 0\}.$$

Now, we consider some conventions for the properties of elements in $CFK^\infty(K)$. If $x \in CFK^\infty(K)$ is in grading (i,j), then Ux is in grading $(i-1,j-1)$. There are two other important gradings associated to an element of $CFK^\infty(K)$.

Definition 4.4. Suppose that $CFK^\infty(K)$ is normalized such that the elements $x = U^0 x$ lie in planar gradings $(0,j)$, i.e. on the j-axis. Then, the *Alexander grading* $A(x)$ of an element $x \in CFK^\infty(K)$ is the j-grading of x.

The *homological grading* $M(x)$ of an element $x \in CFK^\infty(K)$ is determined by the following conventions. The element of $CFK^\infty(K)$ that generates $H_*\big(C\{i=0\},\partial_{\mathrm{vert}}\big)$ has homological grading 0. The boundary map ∂ lowers the homological grading of an element by 1. Multiplication by U lowers the homological grading of an element by 2.

There are many concordance invariants that can be derived from $\mathrm{CFK}^\infty(K)$, including the invariant $V_0(K)$, which is defined as follows.

Definition 4.5. The concordance invariant $V_0(K)$ for a knot K is given by

$$V_0(K) = -\frac{1}{2}\max\{r : \exists x \in H_r(A_0^-) \text{ such that } U^n x \neq 0 \text{ for all n}\}.$$

Here r is the homological grading.

Example 4.6. The complex $\mathrm{CFK}^\infty(K)$, where K is the right-handed trefoil knot 3_1, is shown in Figure 4. The associated graded of $C\{i=0\}$ has Euler characteristic

$$\chi(C\{i=0)\}) = \sum_{j\in\mathbb{Z}} \chi(C_{0,j})t^j = t^{-1}-1+t.$$

So, the Alexander polynomial of the right handed trefoil is $\Delta_{3_1}(t) = t^{-1}-1+t$. The homology of A_0^- is $\mathbb{F}_2[U]\langle[Ua]\rangle$. Thus, $V_0(3_1)$ is $-\frac{1}{2}$ times the homological grading of Ua, which yields

$$V_0(3_1) = -\frac{1}{2}(-2) = 1.$$

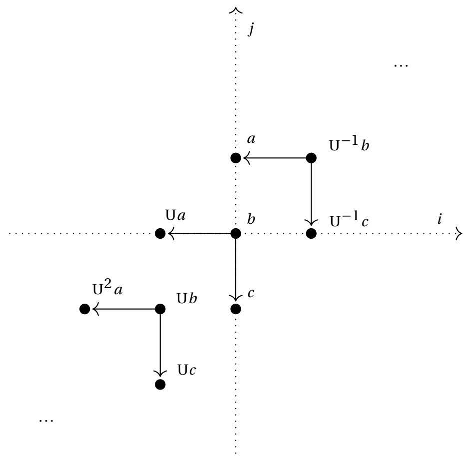

Figure 4: The chain complex $CFK^{\infty}(3_1)$ has three generators, which we call a, b, and c. The arrows in the picture represent the boundary map ∂. The homological grading of a is 0; b has homological grading -1; and c has homological grading -2.

Example 4.7. We now consider the left-handed trefoil knot, which is the mirror of the right-handed trefoil knot. $\mathrm{CFK}^{\infty}(\overline{3_1})$ is shown in Figure 5. The associated graded of $\mathrm{C}\{i=0\}$ has Euler characteristic

$$\chi(\mathrm{C}\{i=0\})) = \sum_{j\in\mathbb{Z}} \chi(\mathrm{C}_{0,j})\, t^j = t^{-1} - 1 + t.$$

So, the Alexander polynomial of the left handed trefoil is $\Delta_{\overline{3_1}}(t) = t^{-1} - 1 + t$. The homology of A_0^- is $\mathbb{F}_2[\mathrm{U}]\langle[\mathrm{U}a + c]\rangle$. Thus, $\mathrm{V}_0(\overline{3_1})$ is $-\frac{1}{2}$ times the homological grading of $\mathrm{U}a + c$, which yields

$$\mathrm{V}_0(\overline{3_1}) = -\frac{1}{2}(0) = 0.$$

Example 4.8. Now we consider $\mathrm{CFK}^{\infty}(\mathrm{K})$, where K is the figure-eight knot 4_1, as shown in Figure 6. The associated graded of $\mathrm{C}\{i=0\}$ has Euler characteristic

$$\chi(\mathrm{C}\{i=0\})) = \sum_{j\in\mathbb{Z}} \chi(\mathrm{C}_{0,j})\, t^j = t^{-1} - 3 + t.$$

So, the Alexander polynomial of the figure eight knot is $\Delta_{4_1}(t) = t^{-1} - 3 + t$. The homology of A_0^- is $\mathbb{F}_2[\mathrm{U}]\langle[x]\rangle \cup [e]$. Thus, $\mathrm{V}_0(4_1)$ is $-\frac{1}{2}$ times the homological grading of x, which yields

$$\mathrm{V}_0(4_1) = -\frac{1}{2}(0) = 0.$$

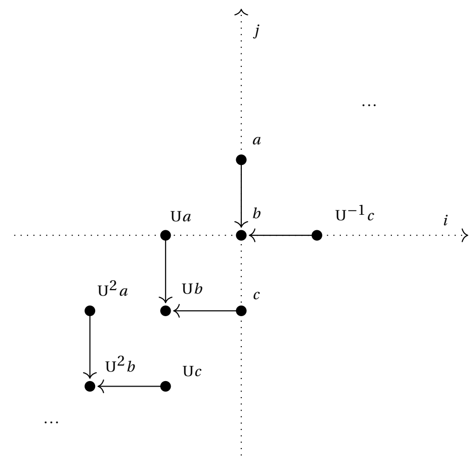

Figure 5: The chain complex $\mathrm{CFK}^\infty(\overline{3_1})$ has three generators, which we call $a, b,$ and c. The homological grading of a is 2; b has homological grading 1; and c has homological grading 0.

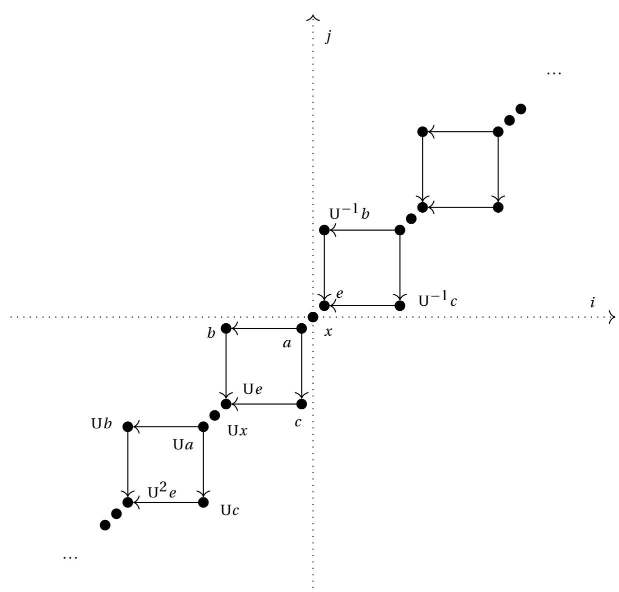

Figure 6: The chain complex $\mathrm{CFK}^\infty(4_1)$ has five generators, which we call a, b, c, e and x. The homological gradings of a, e and x are 0; b has homological grading 1; and c has homological grading -1.

4.2 The involutive concordance invariants

We now introduce the involutive concordance invariants $\underline{V}_0$ and $\overline{V}_0$. We begin by describing an automorphism $\iota_K : CFK^\infty(K) \to CFK^\infty(K)$ for a knot K.

Definition 4.9. For a knot K the *Sarkar involution* $\sigma : CFK^\infty(K) \to CFK^\infty(K)$ is given by

$$\sigma = \mathrm{Id} + U^{-1}(\Phi \circ \Psi),$$

where Id is the identity map on $CFK^\infty(K)$, and $\Phi, \Psi : CFK^\infty(K) \to CFK^\infty(K)$ are the chain maps given as follows. Suppose $x \in CFK^\infty(K)$. Then,

$$\Phi(x) = \sum_{i \text{ odd}} \partial_{i0} x$$

and

$$\Psi(x) = \sum_{j \text{ odd}} \partial_{0j} x.$$

The Sarkar involution is filtered, preserves homological degree, and is an involution up to chain homotopy. We use the Sarkar map to describe the chain map ι_K on $CFK^\infty(K)$ as follows. For a knot K, the map $\iota_K : CFK^\infty(K) \to CFK^\infty(K)$ is an automorphism with the following additional properties:

1. ι_K is a skew-filtered chain map.
2. ι_K preserves homological degree.
3. $\iota_K^2 = \sigma$ up to chain homotopy equivalence.

In many nice cases, although certainly not all, these properties are enough to specify ι_K up to skew-equivariant chain homotopy equivalence. Now, we review the definitions of the involutive concordance invariants.

Definition 4.10. Let AI_0^- be the mapping cone $\mathrm{Cone}(A_0^- \xrightarrow{Q(\iota_K+\mathrm{Id})} QA_0^-[-1])$. Then, the involutive concordance invariants $\underline{V}_0$ and $\overline{V}_0$ are

$$\underline{V}_0 = -\frac{1}{2}\Big(\max\{r : \exists x \in H_r(AI_0^-) \text{ s.t. } U^n x \neq 0 \text{ and } U^n x \notin \mathrm{Im}(Q) \quad \forall n\} - 1\Big),$$

$$\overline{V}_0 = -\frac{1}{2}\max\{r : \exists x \in H_r(AI_0^-) \text{ s.t. } U^n x \neq 0 \quad \forall n \text{ and } \exists m \geq 0 \text{ s.t. } U^m x \in \mathrm{Im}(Q)\},$$

where Im(Q) denotes the image of Q.

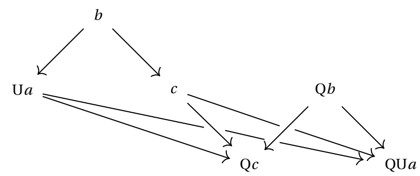

Figure 7: AI_0^- for the right-handed trefoil knot consists of all positive U-powers of the structure shown.

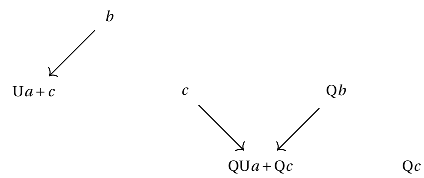

Figure 8: AI_0^- for the right-handed trefoil knot shown after applying a change of basis to the structure in Figure 7.

Example 4.11. Recall that $CFK^\infty(3_1)$ has three generators which we call $a, b,$ and c. The boundary map ∂ is given by $\partial(a) = \partial(c) = 0$ and $\partial(b) = Ua + c$. The map ι_K for $K = 3_1$ is a reflection over the line $i = j$. Concretely, this means that $\iota_{3_1}(a) = U^{-1}c$, $\iota_{3_1}(b) = b$, and $\iota_{3_1}(c) = Ua$. Then, the mapping cone

$$AI_0^- = \mathrm{Cone}(A_0^- \xrightarrow{Q(\iota_{3_1}+\mathrm{Id})} QA_0^-[-1])$$

looks like copies of the structure shown in Figure 7. After a change of basis, AI_0^- has the simplified picture shown in Figure 8. The homology of AI_0^- is

$$\mathbb{F}_2[U]\langle [c + Qb], [Qc] \rangle.$$

$H_*(AI_0^-)$ is a module over $\mathbb{F}_2[U,Q]/Q^2$. So, we can form two towers from the subspaces that generate the homology as shown in Figure 9. We examine the homological gradings of the topmost elements of the towers. The element $c + Qb$ has homological grading -1, while Qc has homological grading -2. Thus, $\underline{V}_0(3_1) = -\frac{1}{2}(-1-1) = 1$ and $\overline{V}_0(3_1) = -\frac{1}{2}(-2) = 1$.

Example 4.12. The involutive concordance invariants for the left-handed trefoil knot can be calculated in a similar way. Recall that $CFK^\infty(\overline{3_1})$ has three generators which we call $a, b,$ and c. The boundary map ∂ is given by $\partial(a) = b, \partial(b) = 0$, and $\partial(c) = Ub$. As with the right handed trefoil, $\iota(\overline{3}_1)$ is a reflection over the line $i = j$. The mapping cone

$$AI_0^- = \mathrm{Cone}(A_0^- \xrightarrow{Q(\iota_{\overline{3}_1}+\mathrm{Id})} QA_0^-[-1])$$

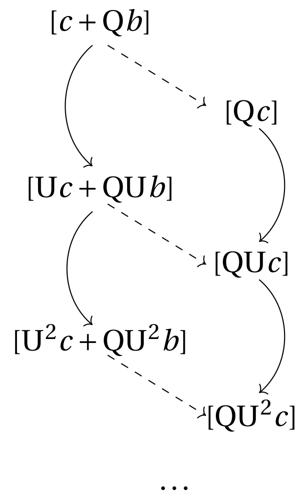

Figure 9: $H_*(AI_0^-)$ for the right-handed trefoil knot can be described by two linked towers. The tower on the left contains no elements in the image of Q, while the tower on the right contains only elements that are in the image of Q. Each tower is organized by increasing powers of U. Curved lines denote multiplication by U, while dashed lines denote application of Q.

has the form shown in Figure 10. The result of changing the basis is shown in Figure 11. The homology of AI_0^- is

$$\mathbb{F}_2[U]\langle [Ua+c], [QUa+Qc]\rangle \cup [b] \cup [Qb].$$

We can form two towers from the subspaces that generate the homology as shown in Figure 12. We examine the homological gradings of the topmost elements of the towers. The element $Ua+c$ has homological grading 1, while b has homological grading 2. Thus, $\underline{V}_0(\overline{3_1}) = -\frac{1}{2}(1-1) = 0$ and $\overline{V}_0(\overline{3_1}) = -\frac{1}{2}(2) = -1$.

Example 4.13. We also find the involutive concordance invariants for the figure-eight knot from Example 4.8. The map ι_K for $K = 4_1$ is given by $\iota_{4_1}(a) = a + x$, $\iota_{4_1}(b) = c$, $\iota_{4_1}(c) = b$,

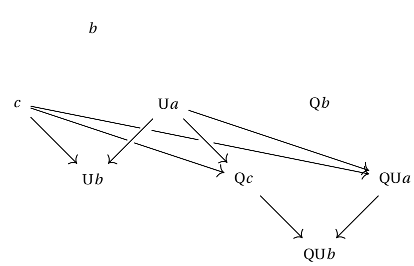

Figure 10: The mapping cone for the left handed trefoil.

$$
\begin{tikzcd}
 & b & & & & & \\
\mathrm{U}a+c & & \mathrm{U}a \arrow[dl] \arrow[drr] & & & \mathrm{Q}b & \\
 & \mathrm{U}b & & & \mathrm{QU}a+\mathrm{Q}c & & \mathrm{Q}c \arrow[dl] \\
 & & & & & \mathrm{QU}b &
\end{tikzcd}
$$

Figure 11: The simplified mapping cone for the left handed trefoil.

$$
\begin{tikzcd}
 & {[b]} \arrow[dd, bend left] & \\
{[\mathrm{U}a+c]} \arrow[dd, bend right] \arrow[dr, dashed] & & {[\mathrm{Q}b]} \\
 & {[\mathrm{QU}a+\mathrm{Q}c]} \arrow[dd, bend left] & \\
{[\mathrm{U}^2a+\mathrm{U}c]} \arrow[dd, bend right] \arrow[dr, dashed] & & \\
 & {[\mathrm{QU}^2a+\mathrm{QU}c]} \arrow[dd, bend left] & \\
{[\mathrm{U}^3a+\mathrm{U}^2c]} \arrow[dr, dashed] & & \\
 & {[\mathrm{QU}^3a+\mathrm{QU}^2c]} & \\
 & \cdots &
\end{tikzcd}
$$

Figure 12: $\mathrm{H}_*(\mathrm{AI}_0^-)$ for the left handed trefoil knot can be described by two linked towers and the stand-alone subspace $[\mathrm{Q}b]$. Note that $\mathrm{QU}b$ is in the image of the differential.

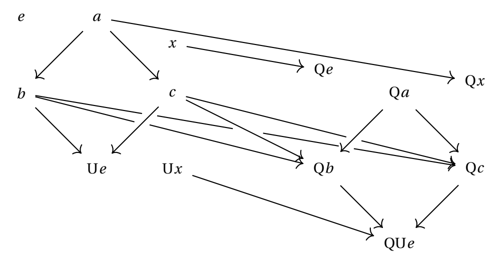

Figure 13: AI_0^- for the figure eight knot consists of the structure shown, and all positive U-translates of the generators $a, b, c, x, Ux, Ue, Qa, Qb, Qc, Qx$, and QUe.

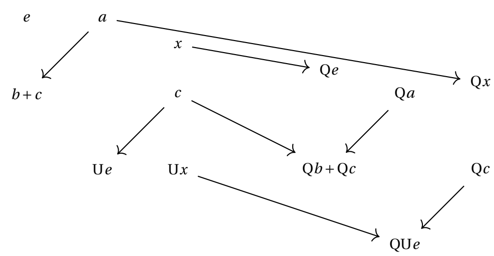

Figure 14: AI_0^- for the figure eight knot shown after applying a change of basis to the structure in Figure 13.

$\iota_{4_1}(e) = e$, and $\iota_{4_1}(x) = e + x$. Then, the mapping cone

$$AI_0^- = \mathrm{Cone}(A_0^- \xrightarrow{Q(\iota_{4_1} + \mathrm{Id})} QA_0^-[-1])$$

is represented by the structure shown in Figure 13. After a change of basis, AI_0^- has the simplified picture shown in Figure 14. The homology of AI_0^- is

$$\mathbb{F}_2[U]\langle [Ux + Qc], [Qx] \rangle \cup [e].$$

Thus, we can form two towers from the subspaces that generate the homology as shown in Figure 15. We examine the homological gradings of the topmost elements of the towers. The element $Ux + Qc$ has homological grading -1, while Qx has homological grading 0. Thus, $\underline{V}_0(4_1) = -\frac{1}{2}(-1-1) = 1$ and $\overline{V}_0(3_1) = -\frac{1}{2}(0) = 0$.

5 Heegaard Diagrams for $(1,1)$ Knots

We can compute $CFK^\infty(K)$ for a (1,1)-knot K using information from a representation of K on the torus, called a Heegaard diagram. Heegaard diagrams for $(1,1)$-knots are uniquely determined by a 4-tuple of integers, described by [Rac15] as follows:

$$
\begin{tikzcd}[column sep=small]
 & & {[e]} \\
 & {[\mathrm{Q}x]} \arrow[dd, bend left] & \\
{[\mathrm{U}x+\mathrm{Q}c]} \arrow[dd, bend right] \arrow[dr, dashed] & & \\
 & {[\mathrm{QU}x]} \arrow[dd, bend left] & \\
{[\mathrm{U}^2x+\mathrm{QU}c]} \arrow[dd, bend right] \arrow[dr, dashed] & & \\
 & {[\mathrm{QU}^2x]} \arrow[dd, bend left] & \\
{[\mathrm{U}^3x+\mathrm{QU}^2c]} \arrow[dr, dashed] & & \\
 & {[\mathrm{QU}^3x]} & \\
 & \cdots &
\end{tikzcd}
$$

Figure 15: $\mathrm{H}_*(\mathrm{AI}_0^-)$ for the figure eight knot can be described by two linked towers and the stand-alone subspace $[e]$.

Definition 5.1. For a (1,1)-knot, there exists a (nonunique) parameterization (k,r,c,s) that describes how the knot lies on the torus, where:

1. There are closed curves α and β such that there are $2k+1$ intersections between α and β, labeled $x_0, x_1, \ldots, x_k, x_{-k}, \ldots, x_{-1}, x_0$. Visualizing the torus as a rectangle with identified sides as in Figure 16, β consists of the top, or equivalently the bottom, of the rectangle, and α is the union of the following arcs. In the following, the words 'left' and 'right' are with respect to the orientation of the curve.

2. There are r loops connecting x_{c-i} to x_{c+i} on the left side of β, for $k-r<i\leq k$. The centermost loop contains the basepoint w.

3. There are r loops connecting $x_{-(c-i)}$ to $x_{-(c+i)}$ on the right side of β, for $k-r<i\leq k$. The centermost loop contains the basepoint z.

4. There are $|s|$ bridges connecting the left side of β at x_i and the right side of β at x_j, where:

   - $c-k+r\leq i<c-k+r+|s|$,
   - $-(c-k+r+|s|)<j\leq -(c-k+r)$, and
   - $i-j=2(c-k+r)+|s|-1$.

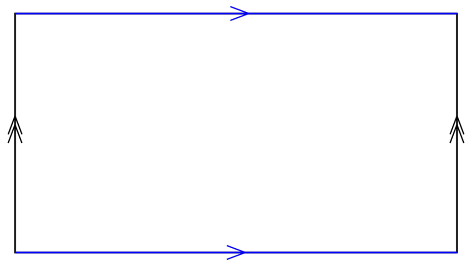

Figure 16: The torus can be represented as a rectangle with opposite sides identified.

5. There are $t = 2(k-r)+1-|s|$ bridges connecting the left side of β at x_i and the right side of β at x_j where:
   - $c+k-r-t < i \leq c+k-r$,
   - $-(c+k-r) \leq j \leq -(c+k-r-t)$, and
   - $i-j = 2(c+k-r)-t+1$.

There is also a *Rasmussen parameterization* for $(1,1)$-knots which is given by a different 4-tuple [Ras05]. A Heegaard diagram for the right-handed trefoil knot 3_1 is shown in Figure 17.

A Heegaard diagram for a (1,1)-knot K determines how K lies on a torus in the following way. The understrand of K is drawn from w to z without intersecting α. Then, the overstrand of K is drawn from z to w without intersecting β. Figure 18 depicts the right-handed trefoil knot on the torus.

We may extract the generators for $CFK^\infty(\mathrm{K})$ from the Heegaard diagram, and identify bigons in the diagram, which determine the boundary map. A *bigon* in the $(1,1)$-diagram for a knot K is a disk on the torus Σ whose boundary consists of one segment from each of the curves α and β such that α and β intersect exactly twice. The disk must be convex at the intersection points, that is, it must occupy one of the four regions of $\Sigma-\alpha-\beta$ which meet at that corner. Examples of bigons are shown in Figures 19, 31, and 32. Bigons determine the boundary map on $CFK^\infty(\mathrm{K})$ in the following way. Given a bigon with intersection points x and y between the curves α and β, we orient the bigon so that the part of the curve β on the boundary is on the left. Assume that with this orientation, x is on the top and y is on the bottom. Suppose the bigon contains m copies of the point z and n copies of the point w. Then, the bigon corresponds to an appearance of the element $\mathrm{U}^n x$ in the boundary of y. Moreover, the difference in Alexander gradings is $\mathrm{A}(x)-\mathrm{A}(y) = m-n$. The difference in homological gradings is $\mathrm{M}(x)-\mathrm{M}(y) = 1-2n$. By taking the sum over all bigons in a Heegaard diagram for a knot K, the differential ∂ on $CFK^\infty(\mathrm{K})$ is determined. An example of this process is carried out in Section 6.2.1.

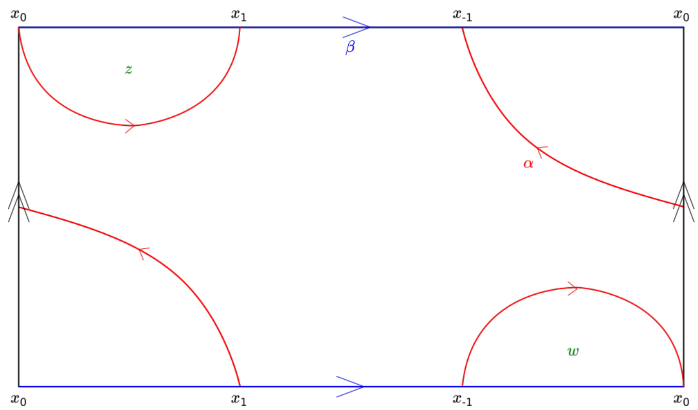

Figure 17: The Heegaard diagram for the right-handed trefoil knot.

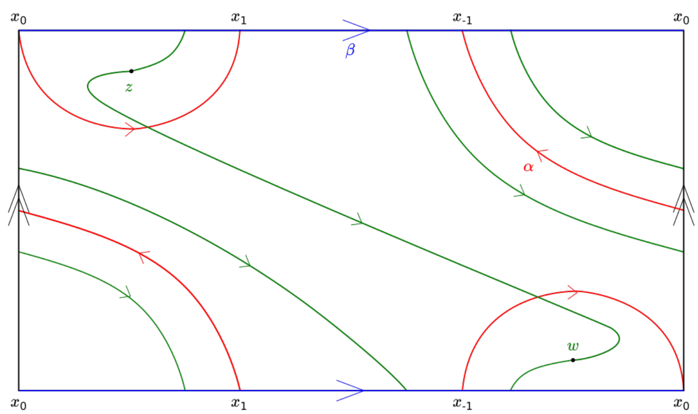

Figure 18: The Heegaard diagram for the right-handed trefoil knot, with the knot shown in green.

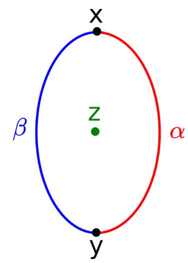

Figure 19: A bigon of this form corresponds to an appearance of the element x in the boundary of y. Furthermore, since the bigon contains a single copy of z, $\mathrm{A}(x)-\mathrm{A}(y)=1$ and $\mathrm{M}(x)-\mathrm{M}(y)=1$.

6 Example Computations of the Involutive Concordance Invariants

We computed the involutive concordance invariants for each of the $(1,1)$-knots included in Table 2 in Section 7. We chose to consider these 10- and 11-crossing (1,1)-knots based on the following classification.

The 10-crossing (1,1)-knots were classified by Morimoto, Sakuma, and Yokota in [MSY96], and the resulting list appears in [GMM05, Table 1]. The knots $10n_{125}$, $10n_{126}$, $10n_{127}$, $10n_{129}$, $10n_{130}$, $10n_{131}$, $10n_{133}$, $10n_{134}$, $10n_{135}$, $10n_{137}$, and $10n_{138}$ are *thin* in the terminology of Heegaard Floer homology. The knot $10n_{124}$ is an L-*space knot* in the terminology of Heegaard Floer homology. The involutive concordance invariants for thin knots and L-space knots have already been determined in [HM17, Section 8]. The remaining knots, $10n_{128}$, $10n_{132}$, $10n_{136}$, $10n_{139}$, $10n_{145}$, and $10n_{161}$, are of interest.

We grouped 11-crossing knots based on whether or not they are *Montesinos*. Montesinos knots are knots composed of rational tangles. Racz classified which 11-crossing non-Montesinos knots are (1,1) in [Rac15, Section 3]. These knots are $11n96$, $11n111$, and $11n135$. These knots are neither thin nor L-space. Klimenko and Sakuma classified which 11-crossing Montesinos knots are (1,1) by showing that they are exactly the 11-crossing Montesinos knots with tunnel number one [KS98, Corollary C]. Castellano-Macías and Owad list all 11-crossing knots with tunnel number one in [CMO21, Appendix A]. Only the non-alternating knots are interesting, since alternating knots are thin. The thin, non-alternating knots on this list are $11n_1$, $11n_2$, $11n_3$, $11n_{13}$, $11n_{14}$, $11n_{15}$, $11n_{16}$, $11n_{17}$, $11n_{18}$, $11n_{28}$, $11n_{29}$, $11n_{30}$, $11n_{51}$, $11n_{52}$, $11n_{53}$, $11n_{54}$, $11n_{55}$, $11n_{56}$, $11n_{58}$, $11n_{59}$, $11n_{60}$, $11n_{62}$, $11n_{63}$, and $11n_{64}$. There are no L-space knots on the list. The knots $11n_{143}$ and $11n_{145}$ are non-Montesinos. So, the remaining knots of interest are $11n_{12}$, $11n_{19}$, $11n_{20}$,

$11n_{38}$, $11n_{57}$, $11n_{61}$, $11n_{70}$, $11n_{79}$, $11n_{102}$, and $11n_{104}$. Thus, we have the final list of 10- and 11-crossing (1,1)-knots for which we calculated the involutive concordance invariants.

The first part of calculating the involutive concordance invariants for the selected (1,1)-knots involved finding a model for $CFK^\infty(\mathrm{K})$ for each knot K. We used one of two strategies to complete this step. For the knots

$$10_{128}, 10_{132}, 10_{136}, 10_{139}, 10_{145}, 11n_{12}, 11n_{19}, 11n_{57}, 11n_{70}, \text{ and } 11n_{79}$$

we used the Heegaard Floer knot homology of each knot given in Section 3 of [BG12] to find $CFK^\infty(\mathrm{K})$; in these cases, this was enough information to specify the full complex up to chain homotopy. For the remaining knots, we used the information in the table in Section 3.7.3 of [Rac15] to draw the $(1,1)$ Heegaard diagram for each knot K, and use this diagram to compute $CFK^\infty(\mathrm{K})$.

6.1 Finding the involutive concordance invariants for $11n_{57}$.

As an example of the first strategy, we consider the computation of $\underline{\mathrm{V}}_0(11n_{57})$ and $\overline{\mathrm{V}}_0(11n_{57})$. The first step is to find $CFK^\infty(11n_{57})$ using the Heegaard Floer knot homology of the knot.

6.1.1 Finding $CFK^\infty(11n_{57})$ using Heegaard Floer knot homology. We detail how to find $CFK^\infty(11n_{57})$, which is shown in Figure 25. The Poincaré polynomial of the knot Floer homology of $11n_{57}$ is given by

$$\widehat{HFK}(\mathrm{S}^3, 11n_{57}) = q^{-7}t^{-4} + 3q^{-6}t^{-3} + 2q^{-5}t^{-2} + q^{-3}t^{-1} + 3q^{-2} + q^{-1}t + 2q^{-1}t^2 + 3t^3 + qt^4,$$

where an entry $q^m t^n$ in the sum denotes a one-dimensional summand in the homology in homological grading m and Alexander grading n. So, the generators of $CFK^\infty(11n_{57})$ are arranged as in Figure 20.

We next inspect the vertical differential. By Lemma 2.1 in Section 2.3 of [Hom14], there exists a vertically simplified basis for $CFK^\infty(11n_{57})$. This means that we may assume that the vertical differential ∂_{vert} cancels the basis elements in pairs, except for the one basis element that generates the vertical homology. Since b, c, and d are the only basis elements that have homological grading 0, one of them must generate the vertical homology. Without loss of generality let c be this element. Then, either $\partial_{\mathrm{vert}}(a) = b$ or $\partial_{\mathrm{vert}}(a) = d$. We choose the first option. Similarly, we choose

$$\partial_{\mathrm{vert}}(j) = k, \partial_{\mathrm{vert}}(l) = n, \partial_{\mathrm{vert}}(m) = o, \text{ and } \partial_{\mathrm{vert}}(p) = q.$$

This results in the incomplete complex shown in Figure 21.

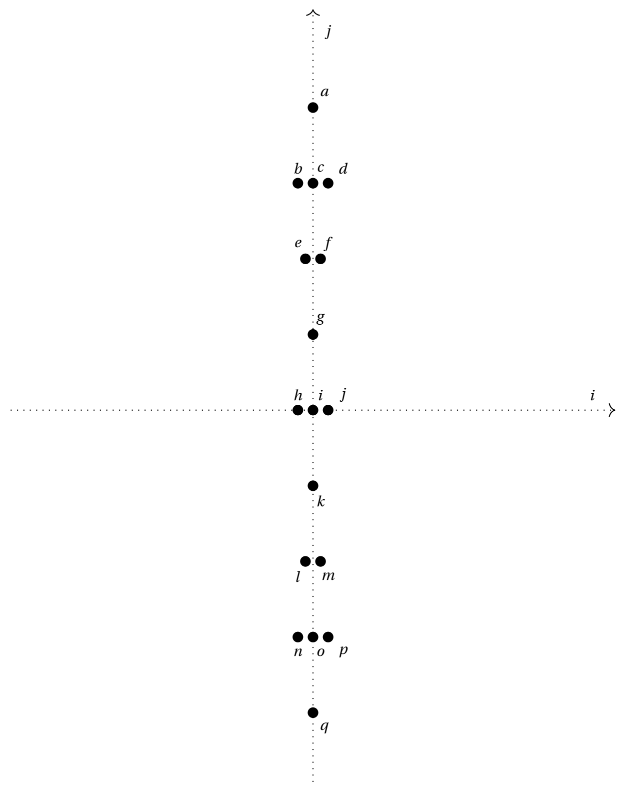

Figure 20: Arrangement of generators of $CFK^{\infty}(11n_{57})$. The homological grading of a is 1; b, c, and d are in homological grading 0; e, g, and g are in homological grading -1; h, i, and j are in homological grading -2; k is in homological grading -3; l and m are in homological grading -5; n, o, and p are in homological grading -6; q has homological grading -7.

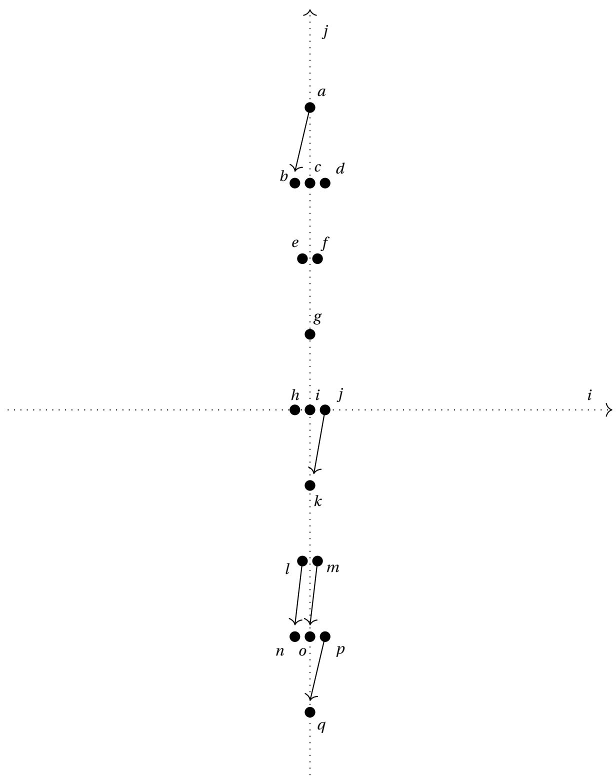

Figure 21: An incomplete picture for $CFK^\infty(11n_{57})$ with part of ∂_{vert} denoted by the arrows. Here $\partial(c) = 0$ and the vertical differentials of the remaining unpaired elements are not yet determined.

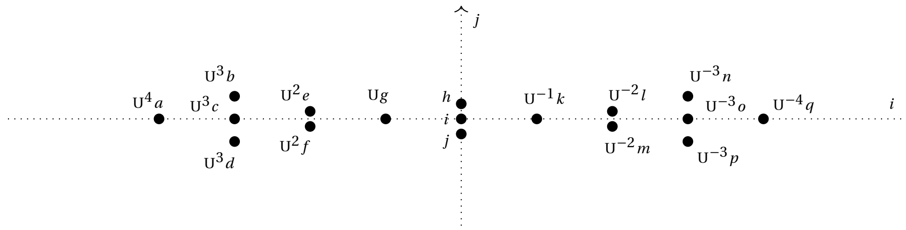

Figure 22: The arrangement of the generators of $C\{j=0\}$. Note that $U^{-3}n, U^{-3}o$, and $U^{-3}p$ all have homological grading 0.

Furthermore, we note that by restrictions from the homological grading, we must have

$$\partial(a) = b, \partial(b) = \epsilon_1 Ua \quad \text{and} \quad \partial(c) = \epsilon_2 Ua,$$

where $\epsilon_1, \epsilon_2 \in \{0,1\}$. Then,

$$\partial^2(b) = \partial(\epsilon_1 Ua) = \epsilon_1 Ub = 0 \quad \text{and} \quad \partial^2(c) = \partial(\epsilon_2 Ua) = \epsilon_2 Ub = 0,$$

which imply that $\epsilon_1 = \epsilon_2 = 0$.

We now consider the horizontal differential ∂_{horz}. The arrangement of the generators of $C\{j=0\}$ is shown in Figure 22. We know that the homology of $C\{j=0\}$ is one-dimensional, and is generated by a linear combination of $U^{-3}n, U^{-3}o$, or $U^{-3}p$. By the restrictions on homological grading we must have $\partial_{\text{horz}}(g) = 0$. Also, U^4a must be in the image of the horizontal differential, which implies that $\partial_{\text{horz}}(d) = Ua$. Then,

$$\partial^2(d) = \partial(Ua) + \partial(\partial_{\text{vert}} d) = Ub + \partial(\partial_{\text{vert}} d),$$

implying that $\partial_{\text{vert}}(d) = f$. Now we can choose $\partial_{\text{vert}}(e) = h$ and $\partial_{\text{vert}}(g) = i$. We can also choose $\partial_{\text{horz}}(e) = Uc$ and $\partial_{\text{horz}}(f) = Ub$. This is because U^3b and U^3c must be in the image of the horizontal differential, so their preimages under this map must be linearly independent combinations of U^2e and U^2f. Up to a change of basis the above choice is the only possibility. Since Ug must be in the image of ∂_{horz}, we choose $\partial_{\text{horz}}(j) = Ug$. Since $U^{-4}q$ does not generate the homology of $C\{j=0\}$, we choose $\partial_{\text{horz}}(q) = Un$. Given these calculations, the updated pictures for $C\{i=0\}$ and $C\{j=0\}$ are in Figure 23 and Figure 24, respectively.

We now find the rest of the horizontal differential. First, we have

$$\partial^2(e) = \partial(Uc + h) = \partial(h) = 0.$$

By restrictions on homological gradings,

$$\partial(i) = \epsilon_1 Ug \quad \text{and} \quad \partial(j) = \epsilon_2 Ug + k,$$

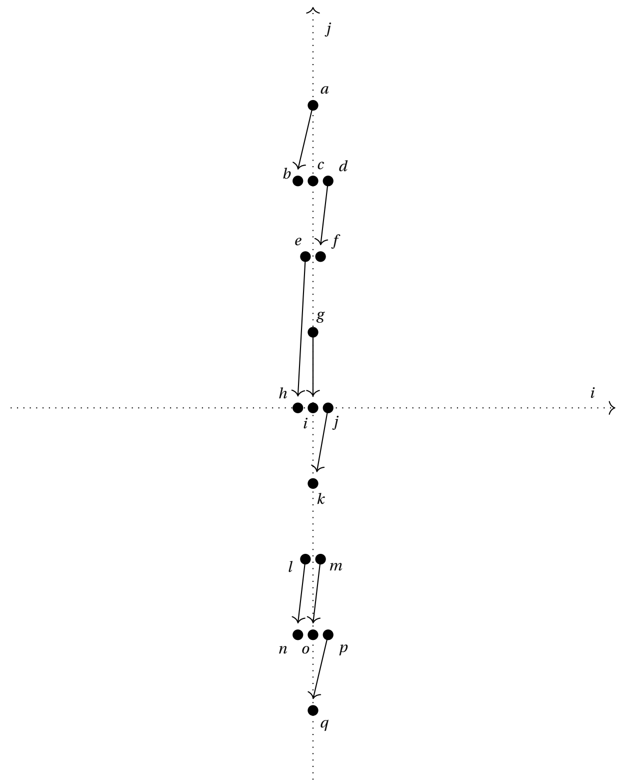

Figure 23: An updated, and now complete picture of $C\{i=0\}$. All generators are paired up by the vertical differential, except for c, which generates the homology of the complex.

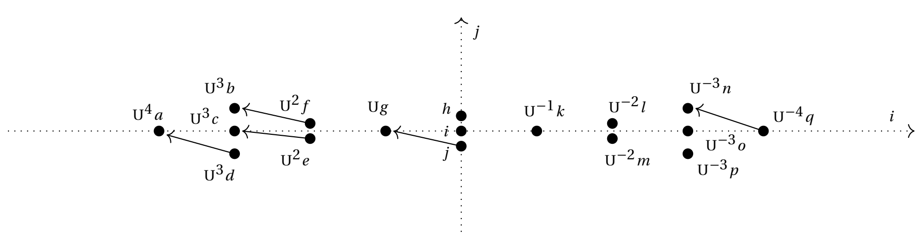

Figure 24: An updated, but incomplete picture for $C\{j=0\}$ with the horizontal differential of U^3d, U^2e, U^2f, j, and $U^{-4}q$ denoted by the arrows.

where $\epsilon_1, \epsilon_2 \in \{0,1\}$. Then,

$$\partial^2(i) = \partial(\epsilon_1 U i) = 0,$$

which implies that $\epsilon_1 = 0$. However, since Ug is in the image of the horizontal, it must be that $\epsilon_2 = 1$. Furthermore,

$$\partial^2(j) = \partial(Ug + k) = Ui + \partial(k) = 0,$$

which implies that $\partial(k) = Ui$. The images of l, m, n, o, p, and q under ∂ are as follows.

$$\begin{aligned} \partial(l) &= n + \kappa_1 U^2 h + \kappa_2 U^2 i + \kappa_3 U^2 j & \partial(n) &= \gamma_1 U l + \gamma_2 U m \\ \partial(m) &= o + \lambda_1 U^2 h + \lambda_2 U^2 i + \lambda_3 U^2 j & \partial(o) &= \beta_1 U l + \beta_2 U m \\ \partial(q) &= \epsilon_1 U n + \epsilon_2 U o + \epsilon_3 U p & \partial(p) &= q + \alpha_1 U l + \alpha_2 U m, \end{aligned}$$

where all coefficients are either 0 or 1. Consider

$$\partial^2(l) = \partial(n + \kappa_1 U^2 h + \kappa_2 U^2 i + \kappa_3 U^2 j) = \gamma_1 U l + \gamma_2 U m + \kappa_3 (U^3 g + U k) = 0.$$

Therefore, $\gamma_1 = \gamma_2 = \kappa_3 = 0$. Similarly,

$$\partial^2(m) = \partial(o + \lambda_1 U^2 h + \lambda_2 U^2 i + \lambda_3 U^2 j) = \beta_1 U l + \beta_2 U m + \lambda_3 (U^3 g + U k) = 0,$$

which implies that $\beta_1 = \beta_2 = \lambda_3 = 0$. So, both $\partial(n)$ and $\partial(o)$ are 0. Thus,

$$\partial^2(q) = \partial(\epsilon_1 U n + \epsilon_2 U o + \epsilon_3 U p) = \epsilon_3 (U q + \alpha_1 U^2 l + \alpha_2 U^2 m),$$

which implies that $\epsilon_3 = 0$. Now, since $\partial_{\text{horz}}(q)$ must be nonzero we have that $\partial(q) = Un$, which is the only option up to relabeling and changing the basis. Lastly we consider

$$\partial^2(p) = \partial(q + \alpha_1 U l + \alpha_2 U m) = U n + \alpha_1 (U n + \kappa_1 U^3 h + \kappa_2 U^3 i) + \alpha_2 (U o + \lambda_1 U^3 h + \lambda_2 U^3 i) = 0.$$

It follows that $\alpha_2 = \kappa_1 = \kappa_2 = 0$ and $\alpha_1 = 1$. Additionally, $\lambda_1 = 1$, because h does not generate the homology of $C\{j = 0\}$. Up to a change of basis we also have $\partial(m) = o + U^2 h$. We have determined the image of all generators of $CFK^\infty(11n_{57})$ under the boundary map. The resulting complex is shown in Figure 25.

6.1.2 Finding the map ι_K for $11n_{57}$.

The complex associated to $11n_{57}$ is shown in Figure 25. All coefficients in the following discussion are either 0 or 1. Since ι_K is skew-filtered and grading-preserving, it must be of the form below.

$$\begin{aligned} a &\mapsto U^{-4} q & b &\mapsto \beta_0 U^{-3} p + \beta_1 U^{-3} o + \beta_2 U^{-3} n \\ c &\mapsto \delta_0 U^{-3} p + \delta_1 U^{-3} o + \delta_2 U^{-3} n & d &\mapsto \alpha_0 U^{-3} p + \alpha_1 U^{-3} o + \alpha_2 U^{-3} n \end{aligned}$$

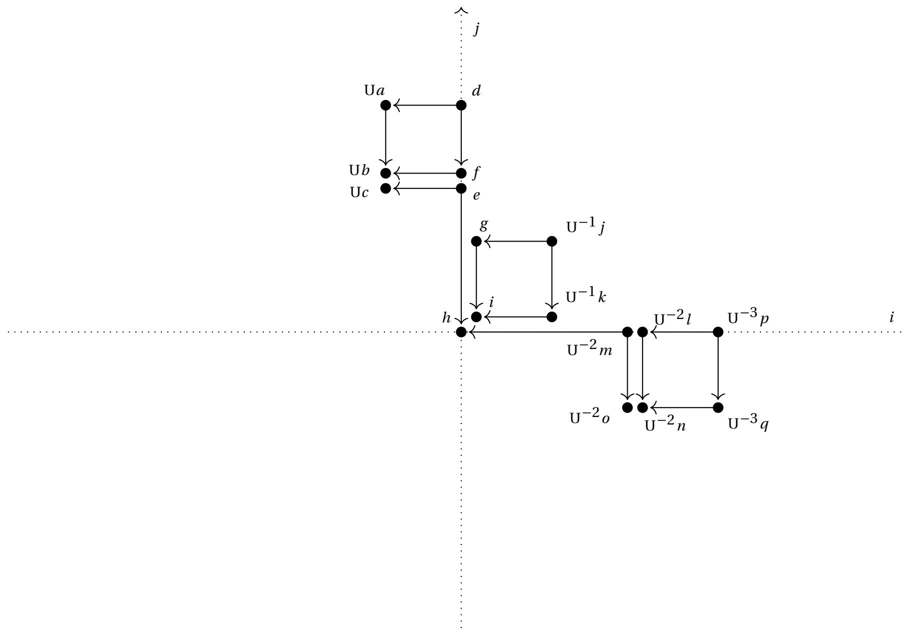

Figure 25: $CFK^{\infty}(11n_{57})$ decomposes as an $\mathbb{F}_2[\mathrm{U},\mathrm{U}^{-1}]$ complex into the direct sum of a staircase and three boxes.

$$
\begin{array}{ll}
e \mapsto \epsilon_0\mathrm{U}^{-1}k+\epsilon_1\mathrm{U}^{-2}m+\epsilon_2\mathrm{U}^{-2}l & f \mapsto \gamma_0\mathrm{U}^{-1}k+\gamma_1\mathrm{U}^{-2}m+\gamma_2\mathrm{U}^{-2}l \\
g \mapsto \mathrm{U}^{-1}k & h \mapsto \eta_0 j+\eta_1\mathrm{U}i+\eta_2 h \\
i \mapsto \psi_0 h+\psi_1 i+\psi_2 j & j \mapsto \zeta_0 j+\zeta_1\mathrm{U}i+\zeta_2 h \\
k \mapsto \mathrm{U}g & l \mapsto \kappa_0\mathrm{U}^2 f+\kappa_1\mathrm{U}^2 e+\kappa_2\mathrm{U}^2 g \\
m \mapsto \theta_0\mathrm{U}^2 f+\theta_1\mathrm{U}^2 e+\theta_2\mathrm{U}^2 g & n \mapsto \nu_0\mathrm{U}^3 d+\nu_1\mathrm{U}^3 b+\nu_2\mathrm{U}^3 c \\
o \mapsto \mu_0\mathrm{U}^3 d+\mu_1\mathrm{U}^3 b+\mu_2\mathrm{U}^3 c & p \mapsto \lambda_0\mathrm{U}^3 d+\lambda_1\mathrm{U}^3 b+\lambda_2\mathrm{U}^3 c \\
q \mapsto \mathrm{U}^4 a. &
\end{array}
$$

Furthermore, since ι_K is a chain map, we can narrow down the options further to conclude that it has the form of the following map.

$$
\begin{array}{ll}
a \mapsto \mathrm{U}^{-4}q & b \mapsto \mathrm{U}^{-3}n \\
c \mapsto \epsilon_1\mathrm{U}^{-3}o+\epsilon_2\mathrm{U}^{-3}n & d \mapsto \mathrm{U}^{-3}p+\alpha_1\mathrm{U}^{-3}o+\alpha_2\mathrm{U}^{-3}n \\
e \mapsto \epsilon_0\mathrm{U}^{-1}k+\epsilon_1\mathrm{U}^{-2}m+\epsilon_2\mathrm{U}^{-2}l & f \mapsto \mathrm{U}^{-2}l \\
g \mapsto \mathrm{U}^{-1}k & h \mapsto \epsilon_0\mathrm{U}i+\epsilon_1 h \\
i \mapsto i & j \mapsto j+\zeta_1\mathrm{U}i+\zeta_2 h \\
k \mapsto \mathrm{U}g & l \mapsto \mathrm{U}^2 f
\end{array}
$$

$$
\begin{aligned}
&m \mapsto \theta_0 U^2 f + \theta_1 U^2 e + \theta_2 U^2 g && n \mapsto U^3 b \\
&o \mapsto \theta_0 U^3 b + \theta_1 U^3 c && p \mapsto U^3 d + \lambda_1 U^3 b + \lambda_2 U^3 c \\
&q \mapsto U^4 a.
\end{aligned}
$$

Now we consider the requirement that $\iota_K^2 = \sigma$ up to chain homotopy equivalence, where σ is the Sarkar involution. Since ι_K and σ are both filtered, and because the boundary map ∂ reduces the homological grading by one, any map $H : CFK^\infty(11n_{57}) \to CFK^\infty(11n_{57})$ such that $\partial H + H\partial = \iota_K^2 + \sigma$ must be filtered and increase homological grading by one where it is nonzero. There is no such map except for the trivial map $H \equiv 0$. Thus, we have $\iota_K^2 = \sigma$. In this case we see that σ is the identity map except at d, j, and p. At these points we have $\sigma(d) = d + b, \sigma(j) = j + i$, and $\sigma(p) = p + n$. Applying this restriction results in a further simplification of the options for ι_K, which is shown below.

$$
\begin{aligned}
&a \mapsto U^{-4} q && b \mapsto U^{-3} n \\
&c \mapsto U^{-3} o + \epsilon_2 U^{-3} n && d \mapsto U^{-3} p + \alpha_1 U^{-3} o + \alpha_2 U^{-3} n \\
&e \mapsto U^{-1} k + U^{-2} m + \epsilon_2 U^{-2} l && f \mapsto U^{-2} l \\
&g \mapsto U^{-1} k && h \mapsto U i + h \\
&i \mapsto i && j \mapsto j + \zeta_1 U i + h \\
&k \mapsto U g && l \mapsto U^2 f \\
&m \mapsto \epsilon_2 U^2 f + U^2 e + U^2 g && n \mapsto U^3 b \\
&o \mapsto \epsilon_2 U^3 b + U^3 c && p \mapsto U^3 d + \lambda_1 U^3 b + \alpha_1 U^3 c \\
&q \mapsto U^4 a.
\end{aligned}
$$

To simplify the possibilities for ι_K we make the following change of basis (and then immediately drop the primes):

$$
\begin{aligned}
m' &= m + \epsilon_2 l \\
o' &= o + \epsilon_2 n \\
p' &= p + \alpha_1 o + \alpha_2 n \\
j' &= j + \zeta_1 U i.
\end{aligned}
$$

As a result ι_K is of the form

$$
\begin{aligned}
&a \mapsto U^{-4} q && b \mapsto U^{-3} n \\
&c \mapsto U^{-3} o && d \mapsto U^{-3} p \\
&e \mapsto U^{-1} k + U^{-2} m && f \mapsto U^{-2} l \\
&g \mapsto U^{-1} k && h \mapsto U i + h
\end{aligned}
$$

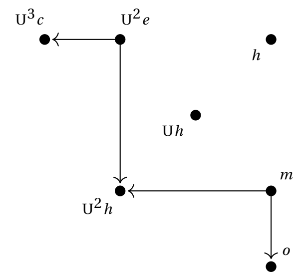

Figure 26: A_0^- for the staircase subcomplex of $CFK^\infty(11n_{57})$ consists of all non-negative U-translates of the staircase shown, along with the elements h and Uh.

$$\begin{aligned} &i \mapsto i && j \mapsto j+h \\ &k \mapsto Ug && l \mapsto U^2 f \\ &m \mapsto U^2e + U^2g && n \mapsto U^3 b \\ &o \mapsto U^3 c && p \mapsto U^3 d + U^3 b \\ &q \mapsto U^4 a. && \end{aligned}$$

All other maps that satisfy the necessary properties of ι_K are equivalent to this solution up to a change of basis. We also see that the boxes in the second and fourth quadrants interact only with each other, and that no other part of the complex interacts with them. Thus, they need not be considered in the calculation of the concordance invariants, since they can be removed as an equivariant summand.

6.1.3 Finding $\underline{V}_0(11n_{57})$ and $\overline{V}_0(11n_{57})$. Using the map ι_K, we may now compute $V_0(11n_{57})$ and the involutive concordance invariants $\overline{V}_0(11n_{57})$ and $\underline{V}_0(11n_{57})$.

To find V_0 it is enough to consider the staircase in $CFK^\infty(11n_{57})$, since the square in the first quadrant has trivial homology. The complex A_0^- for the staircase is shown in Figure 26. The homology of A_0^- is $\mathbb{F}_2[U]\langle[h]\rangle$. Thus, $V_0(11n_{57})$ is $-\frac{1}{2}$ times the homological grading of h, which yields

$$V_0(11n_{57}) = -\frac{1}{2}(-2) = 1.$$

Now we calculate the involutive concordance invariants $\underline{V}_0$ and $\overline{V}_0$. To do so, we need to examine the homology of the mapping cone

$$AI_0^- = \mathrm{Cone}(A_0^- \xrightarrow{Q(\iota_{11n_{57}}+\mathrm{Id})} QA_0^-[-1]).$$

First, we consider A_0^-. The complex A_0^- associated to the subcomplex of $CFK^\infty(11n_{57})$ made up of the staircase and box in quadrant 1 is shown in Figure 27. We also consider the corresponding complex QA_0^-.

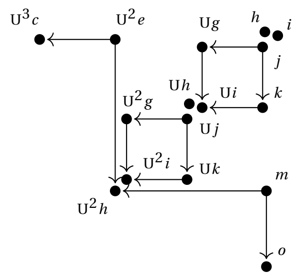

Figure 27: A_0^- for the subcomplex of $CFK^\infty(11n_{57})$ made up of the staircase and box in the first quadrant consists of all non-negative U-translates of the staircase shown, all positive U-translates of the box, and the elements i, h, and Uh.

To simplify the picture and the subsequent calculations we choose the following change of bases (and immediately drop the primes):

$$c' = c + U^{-3}o \qquad Qc' = Qc + QU^{-3}o$$
$$g' = g + U^{-1}k \qquad Qg' = Qg + QU^{-1}k$$
$$e' = e + U^{-2}m \qquad Qe' = Qe + QU^{-2}m.$$

The resulting complex is shown in Figure 28. Now, we look at the map $Q(\iota_{11n_{57}} + \mathrm{Id})$, where $\iota_{11n_{57}}$ is given by the map described at the end of Section 6.1.2. After the change of bases, the restriction of $Q(\iota_{11n_{57}} + \mathrm{Id})$ to the staircase and box in quadrant 1 is given by:

$$c \mapsto 0 \qquad e \mapsto Qg$$
$$g \mapsto 0 \qquad h \mapsto Qi$$
$$i \mapsto 0 \qquad j \mapsto Qh$$
$$k \mapsto QUg \qquad m \mapsto QU^2e + QU^2g + QUk$$
$$o \mapsto QU^3c.$$

Putting all the information together, the complete map on AI_0^- is given by:

$$U^3c \mapsto 0 \qquad QU^3c \mapsto 0$$
$$U^2e \mapsto U^3c + QU^2g \qquad QU^2e \mapsto QU^3c$$
$$Ug \mapsto 0 \qquad QUg \mapsto 0$$

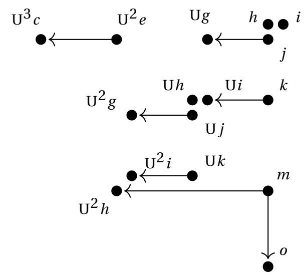

Figure 28: A_0^- for the subcomplex of $CFK^\infty(11n_{57})$ made up of the staircase and box in the first quadrant after a change of basis.

$$\begin{aligned}
&h \mapsto Qi && Qh \mapsto 0\\
&i \mapsto 0 && Qi \mapsto 0\\
&j \mapsto Ug + Qh && Qj \mapsto QUg\\
&k \mapsto Ui + QUg && Qk \mapsto QUi\\
&m \mapsto U^2h + o + QU^2e + QU^2g + QUk && Qm \mapsto QU^2h + Qo\\
&o \mapsto QU^3c && Qo \mapsto 0.
\end{aligned}$$

Now, we can extract the homology of AI_0^-, and form two towers as shown in Figure 29. We examine the homological gradings of the tops of the two towers. The homological grading of $[Qk]$ is -3, while the grading of $[Qh]$ is -2. Thus the involutive concordance invariants are $\underline{V}_0 = 2$ and $\overline{V}_0 = 1$.

6.2 Finding the involutive concordance invariants for 10_{161}.

We now provide a second example, in which we extract $CFK^\infty(10_{161})$ from a (1,1) Heegaard diagram for the knot, then compute the automorphism ι_K and the involutive concordance invariants.

6.2.1 Finding $CFK^\infty(10_{161})$ using a $(1,1)$ Heegaard diagram for 10_{161}.. A $(1,1)$ Heegaard diagram for 10_{161}, computed in [Rac15, Section 3], is shown in Figure 30. We may compute $CFK^\infty(10_{161})$ from Figure 30 by identifying bigons in this Heegaard diagram. Figure 31 and Figure 32 show examples of bigons. Each bigon determines a component of the boundary map for $CFK^\infty(10_{161})$. For the bigon in Figure 31, the curves α and β intersect at x_3 and x_4. When the bigon is oriented such that the segment of β on its boundary is on the right, x_4 is above x_3. Furthermore, the bigon contains one copy of

$$
\begin{tikzcd}
 & & {[i]} \\
 & {[\mathrm{Q}h]} \arrow[dd, bend left] & \\
{[\mathrm{U}h+\mathrm{Q}k]} \arrow[dd, bend right] \arrow[dr, dashed] & & \\
 & {[\mathrm{QU}h]} \arrow[dd, bend left] & \\
{[\mathrm{U}^2h+\mathrm{QU}k]} \arrow[dd, bend right] \arrow[dr, dashed] & & \\
 & {[\mathrm{QU}^2h]} \arrow[dd, bend left] & \\
{[\mathrm{U}^3h+\mathrm{QU}^2k]} \arrow[dr, dashed] & & \\
 & {[\mathrm{QU}^3h]} & \\
 & \cdots &
\end{tikzcd}
$$

Figure 29: $\mathrm{H}_*(\mathrm{AI}_0^-)$ for the knot $11n_{57}$ can be described by two linked towers and the stand-alone subspace $[i]$.

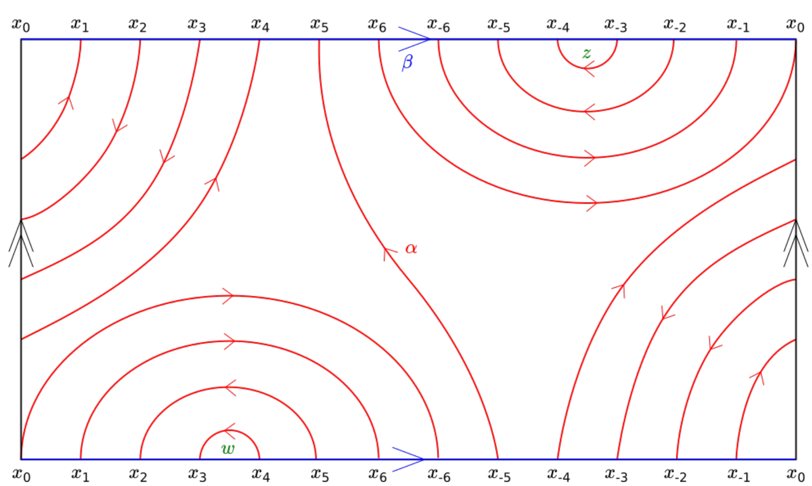

Figure 30: The (1,1)-diagram for 10_{161} has 13 intersection points, labelled by x_i for $-6 \le i \le 6$, between the loops α and β.

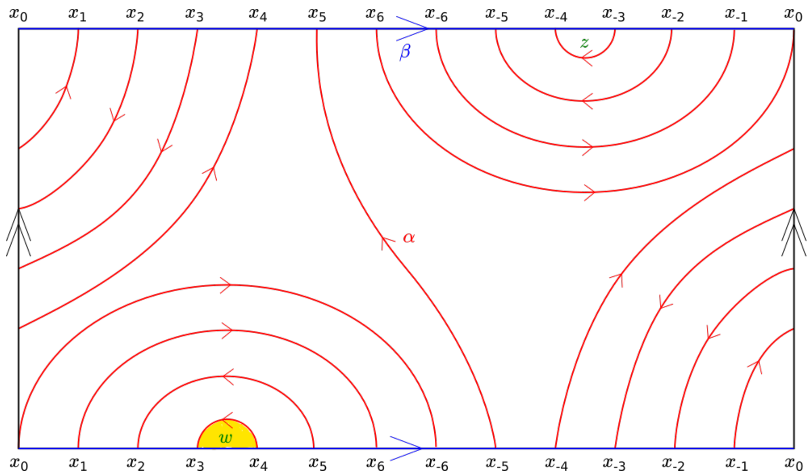

Figure 31: The disk highlighted in yellow is a bigon from x_4 to x_3 containing one copy of w; the corresponding arrow in the chain complex runs from x_4 to Ux_3.

the point w. We conclude that a component of the boundary map for $CFK^\infty(10_{161})$ gives an arrow from x_4 to Ux_3 in the total differential, as shown in Figure 33.

6.2.2 Finding the map ι_K for 10_{161}.

Now, we compute the automorphism ι_K. We make the following change of basis, shown in Figure 34.

$$\begin{aligned}
x_1' &= x_1 + Ux_{-4}\\
x_2' &= x_2 + Ux_{-3}\\
x_5' &= x_5 + x_0\\
x_{-1}' &= x_{-1} + x_4\\
x_{-2}' &= x_{-2} + x_3\\
x_{-5}' &= x_{-5} + x_0
\end{aligned}$$

To reduce the possibilities for ι_K, we follow the same procedure as in Section 6.1.2, where we use that ι_K is skew-filtered, grading-preserving, a chain map, and squares to the Sarkar involution up to filtered chain homotopy. This process yields two possibilities for ι_K. One is the map below, which we will denote ι_K.

$$\begin{aligned}
x_0 &\mapsto x_0 & & \\
x_1' &\mapsto U^{-2}x_{-1}' & \qquad x_{-1}' &\mapsto U^2 x_1'\\
x_2' &\mapsto U^{-1}x_{-2}' & \qquad x_{-2}' &\mapsto Ux_2'\\
x_3 &\mapsto U^2 x_{-3} & \qquad x_{-3} &\mapsto U^{-2}x_3
\end{aligned}$$

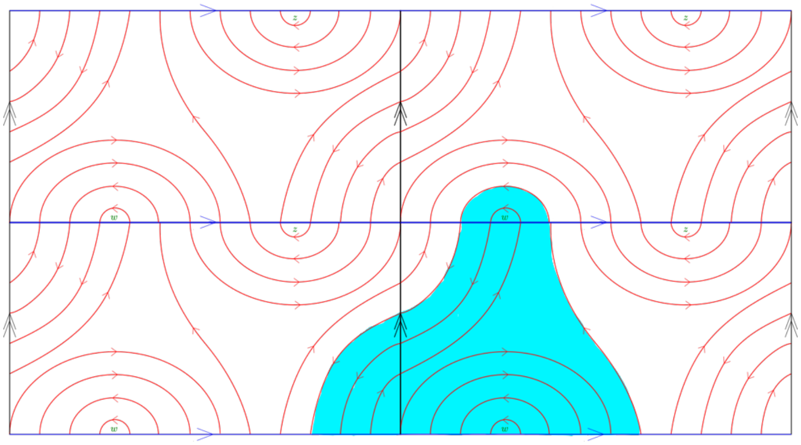

Figure 32: The disk highlighted in blue is a bigon from x_{-5} to x_{-3} containing two copies of w; the corresponding arrow in the chain complex runs from x_{-5} to $U^2 x_{-3}$.

$$
\begin{aligned}
x_4 &\mapsto U^3 x'_{-4} & \qquad x_{-4} &\mapsto U^{-3} x_4\\
x'_5 &\mapsto x'_{-5} & x'_{-5} &\mapsto x'_5\\
x_6 &\mapsto U^{-1} x_{-6} & x_{-6} &\mapsto U x_6 + x'_2
\end{aligned}
$$

The other is the map below, which we will denote ι'_K.

$$
\begin{aligned}
x_0 &\mapsto x_0 & & \\
x'_1 &\mapsto U^{-2} x'_{-1} & \qquad x'_{-1} &\mapsto U^2 x'_1\\
x'_2 &\mapsto U^{-1} x'_{-2} & x'_{-2} &\mapsto U x'_2\\
x_3 &\mapsto U^2 x_{-3} & x_{-3} &\mapsto U^{-2} x_3\\
x_4 &\mapsto U^3 x'_{-4} & x_{-4} &\mapsto U^{-3} x_4\\
x'_5 &\mapsto x'_{-5} & x'_{-5} &\mapsto x'_5\\
x_6 &\mapsto U^{-1} x_{-6} + U^{-1} x_3 & x_{-6} &\mapsto U x_6 + x'_2
\end{aligned}
$$

The maps ι_K and ι'_K are equivalent up to a skew-filtered chain homotopy, the map G below.

$$
\begin{aligned}
x'_1 &\mapsto U^{-1} x_3\\
x_i &\mapsto 0 \text{ for all other generators } x_i
\end{aligned}
$$

for which we have

$$\partial G(x'_1) + G\partial(x'_1) = 0$$

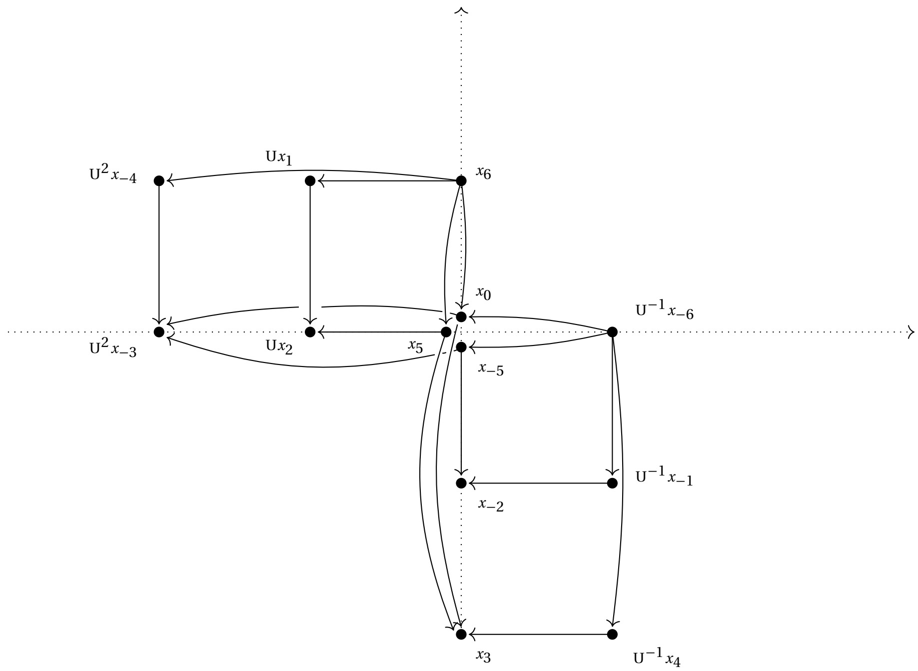

Figure 33: $CFK^{\infty}(10_{161})$ prior to a change of basis.

$$\partial G(x_6) + G\partial(x_6) = G(x_1') = U^{-1}x_3.$$

This is exactly the map $\iota_K - \iota_K'$.

Thus, the two maps ι_K and ι_K' are related by a skew-filtered chain homotopy G, and we may use either in our computation of the involutive concordance invariants for 10_{161}.

6.2.3 Finding $\underline{V}_0(10_{161})$ and $\overline{V}_0(10_{161})$.

Now, we compute the involutive concordance invariants $\overline{V}_0$ and $\underline{V}_0$.

As in the computation of the involutive concordance invariants of $11n_{57}$ in Section 6.1, we examine the homology of the mapping cone

$$AI_0^- = \mathrm{Cone}(A_0^- \xrightarrow{Q(\iota_{10_{161}}+\mathrm{Id})} QA_0^-[-1]).$$

We consider the complex A_0^- associated to the subcomplex in the first quadrant and the corresponding complex QA_0^-. We extract the homology of AI_0^- to form two towers, as shown in Figure 35, then examine the homological gradings of the tops of the two towers. We see that the homological grading of $[Qx_3]$ is 1, the homological grading of $[x_3 + Qx_0]$ is 2, and the homological grading of $[Ux_0 + x_4 + U^3x_{-4}]$ is 1. Thus, $\overline{V}_0(10_{161}) = -1$ and $\underline{V}_0(10_{161}) = 0$.

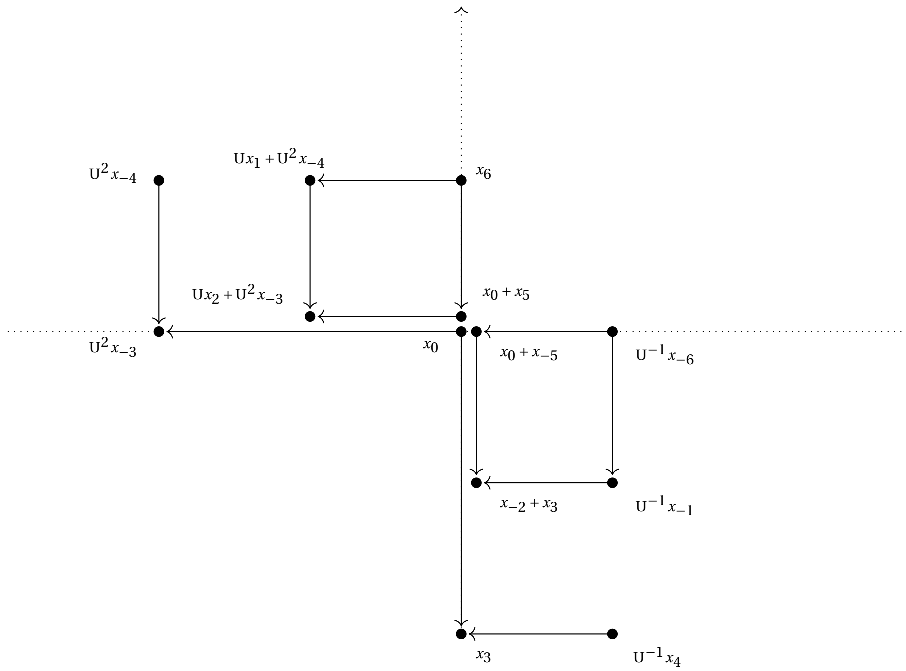

Figure 34: After the change of basis shown, $CFK^{\infty}(10_{161})$ consists of a staircase and two boxes.

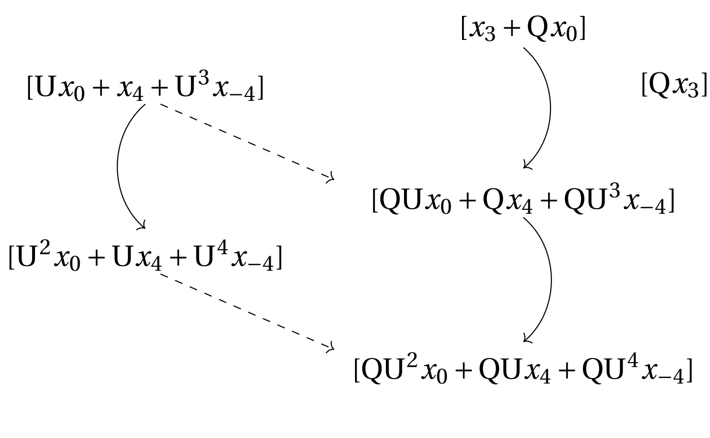

Figure 35: $H_*(AI_0^-)$ for the knot 10_{161} can be written as two towers related by the action of Q and the stand-alone subspace $[Qx_3]$.

7 Results

7.1 Table of Invariants

In Table 2 we show the results of our computations for the involutive concordance invariants for all 10- and 11-crossing (1,1)-knots that are neither thin nor L-space.

Knot K	$\mathbf{V_0(K)}$	$\mathbf{\underline{V}_0(K)}$	$\mathbf{\overline{V}_0(K)}$	$\mathbf{V_0(\overline{K})}$	$\mathbf{\underline{V}_0(\overline{K})}$	$\mathbf{\overline{V}_0(\overline{K})}$
10_{128}	1	1	1	0	0	−1
10_{132}	0	0	−1	1	1	1
10_{136}	0	0	0	0	0	0
10_{139}	2	2	1	0	0	−2
10_{145}	0	0	−1	1	1	1
10_{161}	0	0	−1	1	1	1
$11n_{12}$	1	1	1	0	0	−1
$11n_{19}$	1	1	1	0	0	−1
$11n_{20}$	0	0	0	0	0	0
$11n_{38}$	0	0	−1	1	1	1
$11n_{57}$	1	2	1	0	0	−1
$11n_{61}$	1	1	0	0	0	0
$11n_{70}$	1	1	1	0	0	−1
$11n_{79}$	0	0	0	0	0	0
$11n_{96}$	0	0	−2	2	2	2
$11n_{102}$	0	0	−1	1	1	1
$11n_{104}$	1	1	1	0	0	−1
$11n_{111}$	0	0	0	1	1	0
$11n_{135}$	0	0	−1	1	1	1

Table 2: The involutive concordance invariants $\underline{V}_0$ and $\overline{V}_0$ for the 10- and 11-crossing knots of interest are shown alongside V_0 for comparison.

7.2 Amendments to the literature

In the process of studying the Heegaard diagrams for some of the 11-crossing knots of interest, we discovered a few errors in [Rac15, Section 3.7.3]. In Section 3.7.3, Racz lists parameterizations for the Heegaard diagrams of non-Montesino (1,1)-knots up to 12 crossings. The entries for the knots $12n_{404}$, $12n_{579}$, and $12n_{749}$ do not produce valid diagrams. We found a correct parameterization for $12n_{404}$ by elimination the possibilities based on the Alexander polynomial of the knot. The correct result for $12n_{749}$ is given in [Ras05, Section 6.2]. Table 3 summarizes these two corrections.

Knot	(k, r, c, s)
$12n_{404}$	$(14, 7, -7, 1)$
$12n_{749}$	$(7, 3, -3, 4)$

Table 3: Valid parameterizations for the Heegaard diagrams of $12n_{404}$ and $12n749$

References

[BG12] John A. Balwin and W.D. Gillam, *Computations of Heegaard Floer knot homology*, J. Knot Theory Ramifications **21** (2012), no. 8.

[CMO21] Felipe Castellano-Maciías and Nicholas Owad, *The tunnel number of all 11 and 12 crossing alternating knots*, arXiv:1908.01693, 2021.

[Ghi08] Paolo Ghiggini, *Knot Floer homology detects genus-one fibred knots*, Amer. J. Math. **130** (2008), no. 5, 1151–1169. MR 2450204

[GMM05] Hiroshi Goda, Hiroshi Matsuda, and Takayuki Morifuji, *Knot Floer homology of* $(1,1)$*-knots*, Geom. Dedicata **112** (2005), 197–214. MR 2163899

[HM17] Kristen Hendricks and Ciprian Manolescu, *Involutive Heegaard Floer homology*, Duke Math. J. **166** (2017), no. 7, 1211–1299.

[Hom14] Jennifer Hom, *Bordered Heegaard Floer homology and the tau-invariant of cable knots*, J. Topol. **7** (2014), no. 2, 287–326.

[KS98] Elena Klimenko and Makoto Sakuma, *Two-generator discrete subgroups of* $\mathrm{Isom}(\mathbf{H}^2)$ *containing orientation-reversing elements*, Geom. Dedicata **72** (1998), no. 3, 247–282. MR 1647707

[MSY96] Kanji Morimoto, Makoto Sakuma, and Yoshiyuki Yokota, *Identifying tunnel number one knots*, J. Math. Soc. Japan **48** (1996), no. 4, 667–688. MR 1404816

[Ni07] Yi Ni, *Knot Floer homology detects fibred knots*, ProQuest LLC, Ann Arbor, MI, 2007, Thesis (Ph.D.)–Princeton University. MR 2710002

[OS04a] Peter Ozsváth and Zoltán Szabó, *Heegaard diagrams and holomorphic disks*, Different faces of geometry, Int. Math. Ser. (N. Y.), vol. 3, Kluwer/Plenum, New York, 2004, pp. 301–348.

[OS04b] ______, *Holomorphic disks and knot invariants*, Adv. Math. **186** (2004), no. 1, 58–116.

[OS06] ______, *Holomorphic triangles and invariants for smooth four-manifolds*, Adv. Math. **202** (2006), no. 2, 326–400.

[Rac15] Bela Andras Racz, *Geometry of (1,1)-Knots and Knot Floer Homology*, ProQuest LLC, Ann Arbor, MI, 2015, Thesis (Ph.D.)–Princeton University. MR 3337599

[Ras03] Jacob Andrew Rasmussen, *Floer homology and knot complements*, ProQuest LLC, Ann Arbor, MI, 2003, Thesis (Ph.D.)–Harvard University.

[Ras05] Jacob Rasmussen, *Knot polynomials and knot homologies*, arXiv:math/0504045, 2005.

Anna Antal
anna.antal@yale.edu

Sarah Pritchard
sarah.pritchard@gatech.edu